expression of polyQ-expanded proteins has been reported to upregulate Bax *in vitro*, although a role in polyQ neurotoxicity has never been shown (Chou et al., 2006; Wang et al., 2006). To test the possibility that Bax mediates polyQ-induced neurodegeneration, we cultured primary cortical neurons from *Bax* null mice (Knudson et al., 1995). *Bax* null neurons were completely resistant to AR112 neurotoxicity, demonstrating that apoptosis induced by truncated polyQ-expanded AR requires Bax and is therefore mediated by the intrinsic pathway (Fig. 4*C–E*).

Jun N-terminal kinase activation of c-Jun mediates AR112 neuronal apoptosis

We examined the phosphorylation status of c-Jun in MN-1 cells expressing truncated AR112, and documented production of phospho-c-Jun (Fig. 5*A*). Accumulation of phospho-c-Jun before onset of detectable apoptosis suggests a role for this transcription factor in mediating polyQ-expanded AR toxicity. To test this hypothesis, MN-1 cells were cotransfected with Nt-AR112-GFP and dominant-negative forms of c-Jun. TAM67 is a dominant negative mutant of c-Jun that was generated by removal of the transactivation domain (Chiariello et al., 2000). Coexpression of Nt-AR112-GFP with increasing ratios of TAM67 led to reduced cytotoxicity (Fig. 5*B*). SID-c-Jun is another potent dominant-negative mutant generated by replacing the transactivation domain with the Sin3A-binding domain of Mad (Iavarone et al., 2003). SID-c-Jun yielded a similar reduction in Nt-AR112-GFP cytotoxicity (supplemental Fig. 3*A*, available at www.jneurosci.org as supplemental material). These observations suggested that c-Jun-mediated transcription contributes to polyQ-expanded AR neurotoxicity. We then examined the role of JNK and c-Jun phosphorylation in our primary neuron model, and found that truncated AR112, but not AR19, yielded rapid accumulation of phospho-c-Jun; similar to neurons treated with taxol, a drug that activates the JNK pathway (Fig. 5*C–E*). Phosphorylation of c-Jun occurred at the 18 h time point, well before loss of MAP2 staining, activation of caspase-3, or nuclear condensation. To determine whether JNK activity is required for AR112-induced apoptosis in primary cortical neurons, we pretreated cultures with the JNK inhibitor SP600125 at a concentration specific for JNK (10 μM) (Bennett et al., 2001; Donovan et al., 2002; Bogoyevitch et al., 2004). Pretreatment with the SP600125 kinase inhibitor prevented neurite degeneration, caspase-3 activation, and apoptotic cell death in AR112-transfected neurons (Fig. 5*F*). To confirm that this effect was JNK-dependent, we repeated this experiment with a different JNK inhibitor, and again noted significant reductions in caspase-3 activation, neurite degeneration, and apoptotic cell death in AR112-transfected neurons (supplemental Fig. 3*B*, available at www.jneurosci.org as supplemental material). These results indicated that truncated polyQ-expanded AR activates JNK leading to phosphorylation of c-Jun, which then initiates a Bax-dependent apoptotic cascade. To determine the broader relevance of our findings to polyQ neurodegeneration, we obtained N-terminal truncated huntingtin (htt) expression constructs and transfected them into *Bax* null and control primary cortical neurons. We noted polyQ-htt length-dependent caspase-3 activation and loss of MAP2 immunoreactivity that was almost completely prevented by the absence of Bax (supplemental Fig. 3*C*, available at www.jneurosci.org as supplemental material). N-terminal truncated polyQ-expanded htt expression also elicited marked phosphorylation of c-Jun (supplemental Fig. 3*D*, available at www.jneurosci.org as supplemental material).

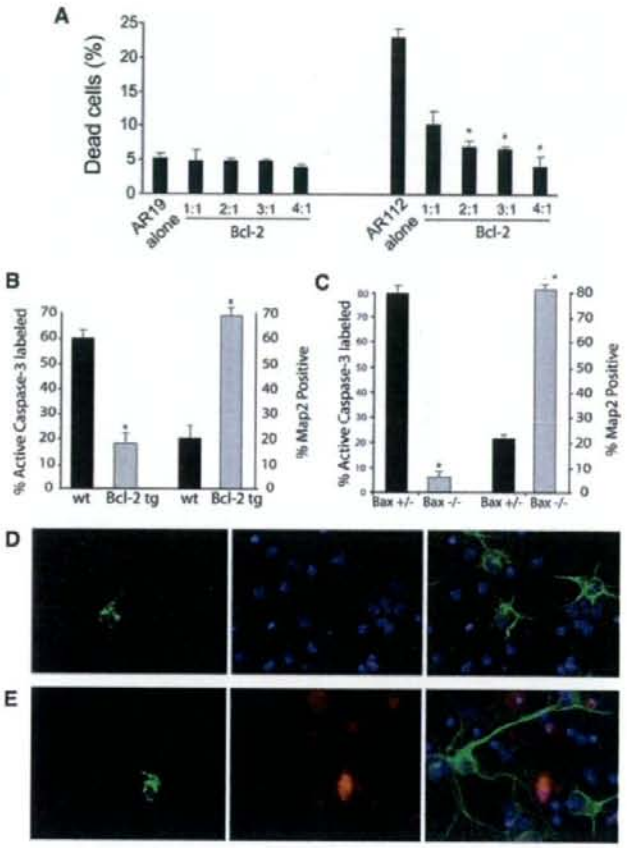

Figure 4. AR112 truncation fragment expression activates apoptosis via the intrinsic pathway. ***A***, *Bcl-2* protects MN-1 cells against AR112-induced cell death (*$p < 0.01$; Student's *t* test). ***B***, Primary cortical neurons derived from *Bcl-2* transgenic mice are strongly protected against AR112 neurotoxicity (*$p < 0.01$; ANOVA). ***C***, Primary cortical neurons derived from *Bax* null mice are fully protected from AR112 neurotoxicity (*$p < 0.01$; ANOVA). ***D***, ***E***, Here we see representative images of AR-transfected neurons using four-channel imaging: DAPI (blue), GFP (green, left), Cy3-labeled active caspase-3 (red), and Cy5-labeled MAP2 (green, right). ***D***, Transfection of Nt-AR112-GFP into *Bax* null neurons does not cause toxicity. Left, We see a neuron expressing AR112. At 24 h after transfection, no active caspase-3 (red) is detected in the AR112-transfected neuron (middle). Cy5 (green) labeling of MAP2 reveals normal, healthy neurites in this AR112-expressing neuron (right). ***E***, Transfection of Nt-AR112-GFP into $Bax^{+/-}$ neurons does produce neurotoxicity. Left, We see a neuron expressing AR112. At 24 h after transfection, immunostaining for active caspase-3 (red) strongly labels this AR112-expressing neuron (middle). While numerous nontransfected cortical neurons exhibit healthy MAP2-positive processes (Cy5, green), the AR112-expressing cortical neuron displays no MAP2 staining (right). In all cases, nuclear condensation indicative of neuron cell death corresponded to caspase-3 activation in these experiments (data not shown).

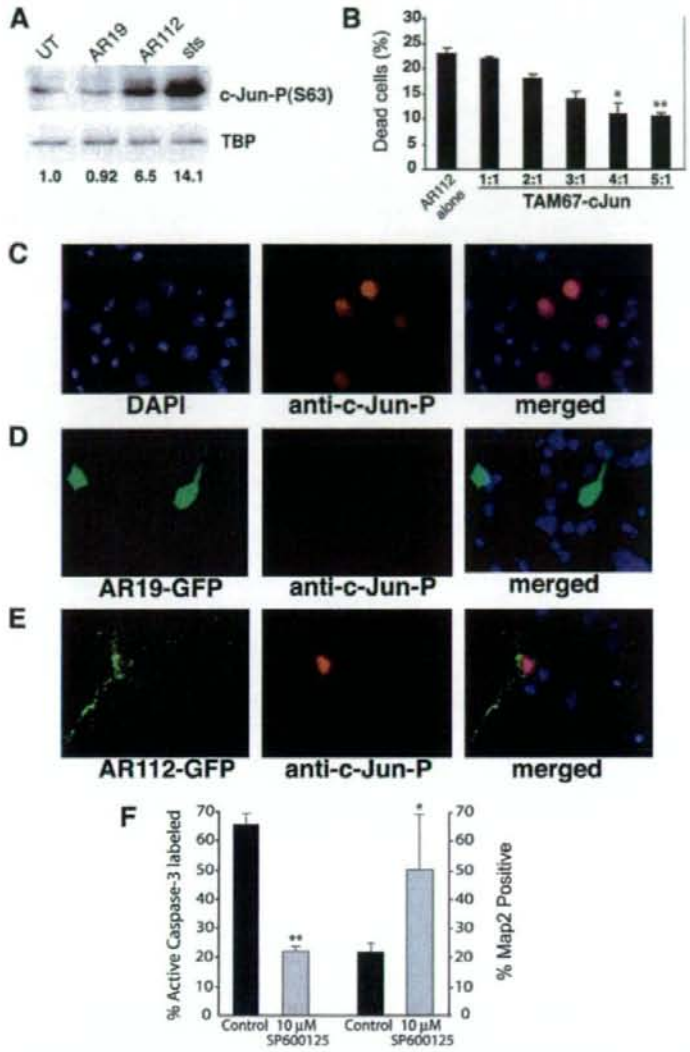

Figure 5. JNK activation of c-Jun mediates polyQ-AR neurotoxicity. ***A***, Western blot analysis for activated (serine-63-phosphorylated) c-Jun in nuclear extracts isolated from untransfected MN-1 cells (UT), AR19-expressing MN-1 cells (AR19), AR112-expressing MN1 cells (AR112), or staurosporine-treated MN-1 cells (sts; positive control). TATA-binding protein (TBP) served as the loading control. The ratio of c-Jun-P(S63):TBP is markedly increased for AR112-expressing MN-1 cells (6.5×) and staurosporine-treated MN-1 cells (14.1×). ***B***, FACS-assisted cell viability assay demonstrates that coexpression of c-Jun dominant-negative TAM67 protects MN-1 cells from AR112 cytotoxicity (*$p < 0.01$, **$p < 0.001$; Student's *t* test). ***C***, Taxol, a positive control for JNK activation of c-Jun, yields numerous anti-c-Jun-P-positive neuron nuclei at 18 h after treatment (DAPI, blue; c-Jun-P, red). ***D***, Primary neurons expressing the AR19 truncation fragment do not display activation of c-Jun-P at 18 h after treatment (AR19-GFP, green; DAPI, blue; c-Jun-P, red). ***E***, Primary neurons expressing AR112 truncation fragment display activation of c-Jun-P at 18 h after treatment (AR112-GFP, green; DAPI, blue; c-Jun-P, red). ***F***, Primary neurons treated with the JNK inhibitor SP600125 are protected from AR112 neurotoxicity (*$p < 0.01$, **$p < 0.001$; ANOVA). In all cases, nuclear condensation indicative of neuron cell death corresponded to caspase-3 activation in these experiments (data not shown).

Truncated AR112 apoptotic activation is mediated by DP5/Hrk

To assess the role of BH3-only proteins in mediating apoptosis induced by polyQ-expanded AR, we obtained *Bim* knock-out mice and *DP5/Hrk* knock-out mice (Putcha et al., 2001; Imaizumi et al., 2004). We transfected cortical neurons from *DP5* null mice and *DP5* heterozygous littermates with Nt-AR19-GFP and Nt-AR112-GFP, quantified caspase-3 activation in AR-expressing neurons, and found that absence of DP5/Hrk provided a partial, yet highly significant degree of protection against AR112-induced apoptosis (Fig. 6*A*). While the degree of protection afforded by the absence of *DP5/Hrk* was only partial, it did approximate the level of protection observed in other single BH3-only knock-out neuron studies (Putcha et al., 2001; Imaizumi et al., 2004). We then performed a similar experiment, this time using primary neurons from *Bim* null mice, but observed no protective effect against AR112 neurotoxicity (Fig. 6*B*). As complete absence of a BH3-only protein in knock-out mice may result in compensatory upregulation of other related BH3-only proteins, we reasoned that acute knock-down experiments were warranted. To evaluate the role of DP5 and Bim in polyQ-AR neurotoxicity, we derived plasmid-based U6 promoter-driven *DP5* shRNA and *Bim* shRNA knock-down constructs. After validating these constructs in neuro2a cells (supplemental Fig. 4*A*,*B*, available at www.jneurosci.org as supplemental material), we cotransfected primary cortical neurons with Nt-AR112-GFP and the *DP5* shRNA knock-down construct or the *Bim* shRNA knock-down, using empty vector as a negative control in each case. *DP5* knock-down yielded an even greater degree of protection from polyQ-AR neurotoxicity (Fig. 6*C*), while *Bim* knock-down again provided no protection against polyQ-AR neurotoxicity (Fig. 6*D*).

As JNK activation results in the transactivation of both Bim and DP5, we decided to measure the expression level of *DP5* in *Bim* null neurons and in *Bim* knock-down neurons. We observed significant upregulation of *DP5* in *Bim* null neurons (Fig. 6*E*), and marked upregulation of *DP5* in *Bim* knock-down neurons (supplemental Fig. 4*C*, available at www.jneurosci.org as supplemental material), suggesting that compensation by *DP5* may account for the lack of Bim null protection. Analysis of *Bim* expression in *DP5* null cortical neurons, however, did not reveal compensatory upregulation of *Bim* (data not shown). Compensatory upregulation of *DP5* in *Bim* null cortical neurons thus led us to derive double knock-out (DKO) mice null for both *Bim* and *DP5/Hrk*. When we transfected DKO cortical neurons with Nt-AR112-GFP expression constructs and scored AR112-expressing neurons for caspase-3 activation and loss of MAP2 immunoreactivity, we found no evidence for protection against AR112-mediated neurotoxicity (Fig. 6*F*). To determine why DKO cortical neurons could not protect against polyQ-AR stress, we examined the expression lev-

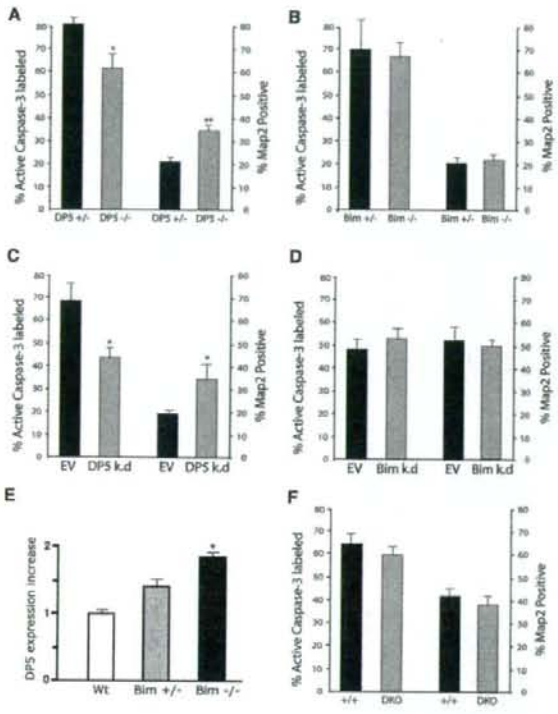

Figure 6. Absence or knock-down of DP5, but not Bim, protects against AR112 neurotoxicity. ***A***, *DP5* null cortical neurons are protected against AR112 neurotoxicity (*$p < 0.01$, **$p < 0.001$; ANOVA). ***B***, *Bim* null status does not protect primary cortical neurons from AR112 neurotoxicity ($p = 0.88$, $p = 0.20$; ANOVA). ***C***, We performed cotransfection of wild-type primary cortical neurons with Nt-AR112 and a *DP5* shRNA expression construct (DP5 k.d.) or empty vector (EV). Knock-down of DP5 significantly protected AR112-expressing neurons from neurotoxicity (*$p < 0.05$; ANOVA). ***D***, Similar cotransfections of wild-type primary cortical neurons with Nt-AR112 and a *Bim* shRNA expression construct (Bim k.d.) yielded no protection against AR-polyQ neurotoxicity ($p = 0.38$, $p = 0.36$; ANOVA). ***E***, Real-time RT-PCR analysis of *DP5* gene expression as a ratio of β-actin gene expression is shown for wild-type (Wt), *Bim* heterozygous null ($Bim^{+/-}$), and *Bim* homozygous null ($Bim^{-/-}$) neurons. Expression of DP5 is significantly increased in $Bim^{-/-}$ neurons compared with either $Bim^{+/-}$ or Wt neurons (*$p < 0.05$; two-tailed *t* test). ***F***, *Bim–DP5* double knock-out (DKO) neurons do not protect against AR112 neurotoxicity ($p = 0.26$, $p = 0.29$; ANOVA).

els of other BH3-only proteins. We documented marked induction of Puma in stressed DKO neurons (supplemental Fig. 5*A*, available at www.jneurosci.org as supplemental material). Indeed, induction of Puma at the protein level was apparent in *Bim* null cortical neurons (supplemental Fig. 5*B*, available at www.jneurosci.org as supplemental material). Evaluation of taxol-induced Noxa activation in Bim null and DKO neurons yielded similar results (data not shown), supporting pronounced compensation of multiple BH3-only proteins in Bim null and DKO mice.

Discussion

One important theme in neurodegeneration has been the recognition of protein misfolding as a common feature (Taylor et al., 2002). Accumulation of misfolded proteins (or peptide fragments thereof) has been linked to endoplasmic reticulum (ER) stress in such disorders (Kouroku et al., 2002; Nishitoh et al., 2002; Rao et al., 2004). In the polyQ diseases, inadequate degradation of misfolded proteins or peptide fragments by the ubiquitin-proteasome system may represent an early step in disease pathogenesis, and likely sets the stage for ER stress activation (Sherman and Goldberg, 2001). Although nuclear localization of polyQ disease proteins appears to be an essential step in disease pathogenesis for HD, SBMA, and SCA1 (Skinner et al., 1997; Saudou et al., 1998; Katsuno et al., 2002), the pathogenic cascade may also involve stress activation pathways in the cytosol (Lindholm et al., 2006; Sekine et al., 2006). To determine the series of molecular steps culminating in cell death in our AR-polyQ models, we began by characterizing the terminal events. Condensed nuclear morphology, DNA laddering, and caspase-3 activation indicated that cellular demise was apoptotic. Apoptosis may be triggered by binding of "death receptors" to activate the caspase-8 dependent extrinsic pathway, or by an intrinsic Bax-dependent pathway culminating in caspase-9 activation (Yuan and Yankner, 2000). Our results revealed that AR polyQ length-dependent cell death is mediated by the intrinsic pathway. Indeed, transfection of N-terminal AR-polyQ into *Bax* null neurons yielded complete protection against AR polyQ length-dependent apoptotic cell death. Previous studies of polyQ neurotoxicity have yielded conflicting data, as one group detected Bax activation in cerebellar neurons expressing either polyQ-expanded ataxin-3 or ataxin-7 (Chou et al., 2006; Wang et al., 2006), while another group reported that isolated polyQ expansion tracts produce nonapoptotic, Bax-independent neurotoxicity in cultured cerebellar neurons (Moulder et al., 1999). Our results, however, indicate that Bax is essential for apoptotic activation in polyQ neurodegeneration, albeit for truncated AR and htt proteins.

As polyQ-expanded proteins are known to elicit ER stress (Kouroku et al., 2002; Nishitoh et al., 2002; Rao et al., 2004), and ER stress has been coupled to JNK activation (Urano et al., 2000), we reasoned that AR polyQ length-dependent cell death would be JNK-dependent, and noted significant protection against AR polyQ neurotoxicity with two different JNK inhibitors (Bennett et al., 2001; Donovan et al., 2002; Holzberg et al., 2003). To delineate the pathway by which AR-polyQ activates apoptosis, we considered how JNK activation could produce Bcl-2 inhibition in neurons. The balance of pro-apoptotic and anti-apoptotic activities of the Bcl-2 family of proteins constitutes a critical checkpoint regulating apoptosis. The "BH3-only" members of the Bcl-2 family are initiators of programmed cell death and stress-induced apoptosis mediated by the mitochondrial pathway (Huang and Strasser, 2000). The BH3-only proteins function by antagonizing anti-apoptotic Bcl-2, Mcl-1, and Bcl-x_L, leading to Bax and/or Bak-dependent loss of mitochondrial membrane integrity. As Bim and DP5/Hrk are activated downstream of JNK and c-Jun in neuronal apoptosis (Inohara et al., 1997; Imaizumi et al., 1999; Harris and Johnson, 2001; Putcha et al., 2001; Whitfield et al., 2001; Imaizumi et al., 2004), we hypothesized that AR-polyQ neuron cell death might be mediated by these BH3-only proteins. DP5/Hrk is a particularly attractive candidate, as it has been implicated in neuron death both in *DP5* null mice and in human ALS patients (Imaizumi et al., 1997; Shinoe et al., 2001; Imaizumi et al., 2004). *DP5* null status conferred significant protection against AR-polyQ neurotoxicity, akin to the level of protection afforded in other stress paradigms performed in single BH3-only knock-out neurons (Putcha et al., 2001; Imaizumi et al., 2004). Absence of Bim, however, did not yield protection against AR-polyQ in primary neurons. We attributed this lack of Bim protection to compensatory upregulation of other BH3-only proteins, as we documented increased DP5/Hrk expression in both *Bim* null neurons and in acute *Bim* shRNA knock-down experiments. Interestingly, *Bim – DP5* DKO cortical neurons also could not protect against AR polyQ stress. Although the basis for

this lack of protection was unclear, significant compensatory upregulation of yet another BH3-only protein, Puma, may account, at least in part, for this observation. Markedly pronounced compensation of BH3-only proteins in *Bim* null neurons is consistent with an emerging view of Bim as a key regulator of intrinsic pathway activation and as a sensor of ER stress (Puthalakath et al., 2007; Willis et al., 2007); hence, a role for Bim in mediating polyQ-AR apoptotic activation cannot be excluded by this study. Nonetheless, our results clearly implicate DP5/Hrk in AR polyQ length-dependent apoptotic activation, suggesting DP5/Hrk upregulation could be involved in SBMA disease pathogenesis. To our knowledge, this investigation is the first to directly document a role for a BH3-only protein in polyQ neurodegeneration.

In this study, we found that expression of an N-terminal AR fragment produced polyQ length-dependent neurodegeneration and cell death in MN-1 motor neuron-like cells and in primary neurons. While the role of N-terminal truncation fragments in some polyQ diseases may be unclear, evidence for the existence of pathogenic N-terminal truncation fragments in SBMA is strong. The pathologic hallmark of SBMA is the presence of both cytoplasmic and nuclear AR inclusions that are detectable in motor neurons of the brainstem and spinal cord, neurons of the dorsal root ganglia, and peripheral tissues including the skin, testis and other visceral organs (Li et al., 1998a,b; Adachi et al., 2005). These inclusions are detected by antibodies that recognize the N terminus of the AR protein, but not by antibodies against the middle or C terminus, suggesting that the C terminus of AR is truncated or masked. Mouse and *Drosophila* models of SBMA in which full-length, polyQ-expanded AR is expressed are also characterized by AR inclusions recognized by antibodies against the N terminus of AR (Takeyama et al., 2002; Walcott and Merry, 2002; Chevalier-Larsen et al., 2004). Extraction of AR protein from affected tissues in these animals, followed by immunoblotting, demonstrates the accumulation of N-terminal fragments that correlate with disease progression (Takeyama et al., 2002; Li et al., 2007). These results strongly suggest that AR truncation, rather than epitope masking, is the basis for detection of N-terminal AR epitopes in SBMA patient tissue and animal models. Moreover, there is extensive evidence that an N-terminal truncation product mediates the cytotoxicity observed in SBMA (Kobayashi et al., 1998; Merry et al., 1998; Ellerby et al., 1999b; Li et al., 2007).

To assess the relevance of our findings to other polyQ diseases involving "toxic fragments," we transfected N-terminal truncated polyQ-huntingtin (htt) into primary cortical neurons from wild-type and Bax null mice. N-terminal polyQ-htt protein accumulated in the cytosol, yielded caspase-3 activation and neurodegeneration, and was Bax-dependent, akin to polyQ-AR. In HD, the necessity of proteolytic cleavage for disease pathogenesis is supported by absence of neurodegeneration in HD YAC transgenic mice expressing htt-128Q with a caspase cleavage site mutation at amino acid position 586 (Graham et al., 2006). Subsequent studies have suggested that htt cleavage is mediated by caspase-6 in the nucleus, and that htt truncation fragments move out of the nucleus into the cytosol (Warby et al., 2008). In SCA3, proteolytic cleavage of polyQ-ataxin-3 enhances misfolding and neurotoxicity in neuroblastoma cells and transgenic mice by yielding a C-terminal polyQ-ataxin-3 fragment (Haacke et al., 2006; Colomer Gould et al., 2007), but the cleavage enzyme, subcellular site of cleavage, and cellular toxicity process remain unknown.

An unresolved question in the neurodegenerative disease field is the contribution of apoptosis to neuron dysfunction and cell death. While considerable evidence exists for prominent activation of apoptotic pathways in degenerating neurons from patients with neurodegenerative disorders (for review, see Mattson, 2000; Yuan and Yankner, 2000), evidence for neuron death mediated by apoptosis is scant in both patient material and animal models (Turmaine et al., 2000; Conforti et al., 2007). Why is this the case? As postmitotic neurons wired into complex synaptic pathways are difficult, if not impossible, to replace, many "brakes," including anti-apoptotic factors such as XIAP and NAIP, prevent the loss of neurons in the face of apoptotic activation (Perrelet et al., 2002). Indeed, modifications of classic apoptosis pathways may explain the cell death process in neurons (Sperandio et al., 2000; Okada and Mak, 2004). However, even if diseased neurons do not die by classic apoptosis, activation of apoptotic mediators could play a crucial role in the pathogenic cascade. For example, elaboration of caspases and other proteolytic enzymes downstream of the JNK activation pathway may be an early and crucial step in the production of misfolded toxic peptides. In AD and HD, mouse models expressing disease mutations do not become affected when disease proteins contain second site mutations at putative caspase cleavage sites (Galvan et al., 2006; Graham et al., 2006). Other *in vivo* studies in mice similarly point to a contribution of active caspases and other apoptotic mediators in disease pathogenesis (Ona et al., 1999; Yuan and Yankner, 2000). In ALS, crossing SOD1 mutant mice with Bcl-2-overexpressing transgenic mice significantly retards disease progression (Kostic et al., 1997). Our findings support the view that apoptotic activation contributes to SBMA disease pathogenesis. Furthermore, the delineation of the JNK–c-Jun-phosporylation–DP5–Bcl-2–Bax pathway in AR polyQ neurotoxicity provides us with a framework to investigate how these events intertwine with ligand dependency, proteolytic cleavage, and subcellular localization. If cross talk does exist between this pathway and key processes of AR polyQ neurotoxicity, then rational decisions about how to pursue therapy for SBMA should be possible.

References

Adachi H, Katsuno M, Minamiyama M, Waza M, Sang C, Nakagomi Y, Kobayashi Y, Tanaka F, Doyu M, Inukai A, Yoshida M, Hashizume Y, Sobue G (2005) Widespread nuclear and cytoplasmic accumulation of mutant androgen receptor in SBMA patients. Brain 128:659–670.

Bennett BL, Sasaki DT, Murray BW, O'Leary EC, Sakata ST, Xu W, Leisten JC, Motiwala A, Pierce S, Satoh Y, Bhagwat SS, Manning AM, Anderson DW (2001) SP600125, an anthrapyrazolone inhibitor of Jun N-terminal kinase. Proc Natl Acad Sci U S A 98:13681–13686.

Bogoyevitch MA, Boehm I, Oakley A, Ketterman AJ, Barr RK (2004) Targeting the JNK MAPK cascade for inhibition: basic science and therapeutic potential. Biochim Biophys Acta 1697:89–101.

Chevalier-Larsen ES, O'Brien CJ, Wang H, Jenkins SC, Holder L, Lieberman AP, Merry DE (2004) Castration restores function and neurofilament alterations of aged symptomatic males in a transgenic mouse model of spinal and bulbar muscular atrophy. J Neurosci 24:4778–4786.

Chiariello M, Marinissen MJ, Gutkind JS (2000) Multiple mitogen-activated protein kinase signaling pathways connect the cot oncoprotein to the c-jun promoter and to cellular transformation. Mol Cell Biol 20:1747–1758.

Chou AH, Yeh TH, Kuo YL, Kao YC, Jou MJ, Hsu CY, Tsai SR, Kakizuka A, Wang HL (2006) Polyglutamine-expanded ataxin-3 activates mitochondrial apoptotic pathway by upregulating Bax and downregulating Bcl-xL. Neurobiol Dis 21:333–345.

Colomer Gould VF, Goti D, Pearce D, Gonzalez GA, Gao H, Bermudez de Leon M, Jenkins NA, Copeland NG, Ross CA, Brown DR (2007) A mutant ataxin-3 fragment results from processing at a site N-terminal to amino acid 190 in brain of Machado-Joseph disease-like transgenic mice. Neurobiol Dis 27:362–369.

Conforti L, Adalbert R, Coleman MP (2007) Neuronal death: where does the end begin? Trends Neurosci 30:159–166.

Cooper JK, Schilling G, Peters MF, Herring WJ, Sharp AH, Kaminsky Z, Masone J, Khan FA, Delanoy M, Borchelt DR, Dawson VL, Dawson TM, Ross CA (1998) Truncated N-terminal fragments of huntingtin with expanded glutamine repeats form nuclear and cytoplasmic aggregates in cell culture. Hum Mol Genet 7:783–790.

Darrington RS, Butler R, Leigh PN, McPhaul MJ, Gallo JM (2002) Ligand-dependent aggregation of polyglutamine-expanded androgen receptor in neuronal cells. Neuroreport 13:2117–2120.

Donovan N, Becker EB, Konishi Y, Bonni A (2002) JNK phosphorylation and activation of BAD couples the stress-activated signaling pathway to the cell death machinery. J Biol Chem 277:40944–40949.

Ellerby LM, Andrusiak RL, Wellington CL, Hackam AS, Propp SS, Wood JD, Sharp AH, Margolis RL, Ross CA, Salvesen GS, Hayden MR, Bredesen DE (1999a) Cleavage of atrophin-1 at caspase site aspartic acid 109 modulates cytotoxicity. J Biol Chem 274:8730–8736.

Ellerby LM, Hackam AS, Propp SS, Ellerby HM, Rabizadeh S, Cashman NR, Trifiro MA, Pinsky L, Wellington CL, Salvesen GS, Hayden MR, Bredesen DE (1999b) Kennedy's disease: caspase cleavage of the androgen receptor is a crucial event in cytotoxicity. J Neurochem 72:185–195.

Galvan V, Gorostiza OF, Banwait S, Ataie M, Logvinova AV, Sitaraman S, Carlson E, Sagi SA, Chevallier N, Jin K, Greenberg DA, Bredesen DE (2006) Reversal of Alzheimer's-like pathology and behavior in human APP transgenic mice by mutation of Asp664. Proc Natl Acad Sci U S A 103:7130–7135.

Garden GA, Libby RT, Fu YH, Kinoshita Y, Huang J, Possin DE, Smith AC, Martinez RA, Fine GC, Grote SK, Ware CB, Einum DD, Morrison RS, Ptacek LJ, Sopher BL, La Spada AR (2002) Polyglutamine-expanded ataxin-7 promotes non-cell-autonomous Purkinje cell degeneration and displays proteolytic cleavage in ataxic transgenic mice. J Neurosci 22:4897–4905.

Goldberg YP, Nicholson DW, Rasper DM, Kalchman MA, Koide HB, Graham RK, Bromm M, Kazemi-Esfarjani P, Thornberry NA, Vaillancourt JP, Hayden MR (1996) Cleavage of huntingtin by apopain, a proapoptotic cysteine protease, is modulated by the polyglutamine tract. Nat Genet 13:442–449.

Graham RK, Deng Y, Slow EJ, Haigh B, Bissada N, Lu G, Pearson J, Shehadeh J, Bertram L, Murphy Z, Warby SC, Doty CN, Roy S, Wellington CL, Leavitt BR, Raymond LA, Nicholson DW, Hayden MR (2006) Cleavage at the caspase-6 site is required for neuronal dysfunction and degeneration due to mutant huntingtin. Cell 125:1179–1191.

Haacke A, Broadley SA, Boteva R, Tzvetkov N, Hartl FU, Breuer P (2006) Proteolytic cleavage of polyglutamine-expanded ataxin-3 is critical for aggregation and sequestration of non-expanded ataxin-3. Hum Mol Genet 15:555–568.

Harris CA, Johnson EM Jr (2001) BH3-only Bcl-2 family members are coordinately regulated by the JNK pathway and require Bax to induce apoptosis in neurons. J Biol Chem 276:37754–37760.

Holzberg D, Knight CG, Dittrich-Breiholz O, Schneider H, Dörrie A, Hoffmann E, Resch K, Kracht M (2003) Disruption of the c-JUN-JNK complex by a cell-permeable peptide containing the c-JUN delta domain induces apoptosis and affects a distinct set of interleukin-1-induced inflammatory genes. J Biol Chem 278:40213–40223.

Huang DC, Strasser A (2000) BH3-only proteins—essential initiators of apoptotic cell death. Cell 103:839–842.

Iavarone C, Catania A, Marinissen MJ, Visconti R, Acunzo M, Tarantino C, Carlomagno MS, Bruni CB, Gutkind JS, Chiariello M (2003) The platelet-derived growth factor controls c-myc expression through a JNK- and AP-1-dependent signaling pathway. J Biol Chem 278:50024–50030.

Ikeda H, Yamaguchi M, Sugai S, Aze Y, Narumiya S, Kakizuka A (1996) Expanded polyglutamine in the Machado-Joseph disease protein induces cell death in vitro and in vivo. Nat Genet 13:196–202.

Imaizumi K, Tsuda M, Imai Y, Wanaka A, Takagi T, Tohyama M (1997) Molecular cloning of a novel polypeptide, DP5, induced during programmed neuronal death. J Biol Chem 272:18842–18848.

Imaizumi K, Morihara T, Mori Y, Katayama T, Tsuda M, Furuyama T, Wanaka A, Takeda M, Tohyama M (1999) The cell death-promoting gene DP5, which interacts with the BCL2 family, is induced during neuronal apoptosis following exposure to amyloid beta protein. J Biol Chem 274:7975–7981.

Imaizumi K, Benito A, Kiryu-Seo S, Gonzalez V, Inohara N, Lieberman AP, Kiyama H, Nuñez G, Leiberman AP (2004) Critical role for DP5/Harakiri, a Bcl-2 homology domain 3-only Bcl-2 family member, in axotomy-induced neuronal cell death. J Neurosci 24:3721–3725.

Inohara N, Ding L, Chen S, Núñez G (1997) *harakiri*, a novel regulator of cell death, encodes a protein that activates apoptosis and interacts selectively with survival-promoting proteins Bcl-2 and Bcl-X(L). EMBO J 16:1686–1694.

Katsuno M, Adachi H, Kume A, Li M, Nakagomi Y, Niwa H, Sang C, Kobayashi Y, Doyu M, Sobue G (2002) Testosterone reduction prevents phenotypic expression in a transgenic mouse model of spinal and bulbar muscular atrophy. Neuron 35:843–854.

Kennedy WR, Alter M, Sung JH (1968) Progressive proximal spinal and bulbar muscular atrophy of late onset. A sex-linked recessive trait. Neurology 18:671–680.

Knudson CM, Tung KS, Tourtellotte WG, Brown GA, Korsmeyer SJ (1995) Bax-deficient mice with lymphoid hyperplasia and male germ cell death. Science 270:96–99.

Kobayashi Y, Miwa S, Merry DE, Kume A, Mei L, Doyu M, Sobue G (1998) Caspase-3 cleaves the expanded androgen receptor protein of spinal and bulbar muscular atrophy in a polyglutamine repeat length-dependent manner. Biochem Biophys Res Commun 252:145–150.

Kostic V, Jackson-Lewis V, de Bilbao F, Dubois-Dauphin M, Przedborski S (1997) Bcl-2: prolonging life in a transgenic mouse model of familial amyotrophic lateral sclerosis. Science 277:559–562.

Kouroku Y, Fujita E, Jimbo A, Kikuchi T, Yamagata T, Momoi MY, Kominami E, Kuida K, Sakamaki K, Yonehara S, Momoi T (2002) Polyglutamine aggregates stimulate ER stress signals and caspase-12 activation. Hum Mol Genet 11:1505–1515.

La Spada AR, Taylor JP (2003) Polyglutamines placed into context. Neuron 38:681–684.

La Spada AR, Wilson EM, Lubahn DB, Harding AE, Fischbeck KH (1991) Androgen receptor gene mutations in X-linked spinal and bulbar muscular atrophy. Nature 352:77–79.

Li M, Miwa S, Kobayashi Y, Merry DE, Yamamoto M, Tanaka F, Doyu M, Hashizume Y, Fischbeck KH, Sobue G (1998a) Nuclear inclusions of the androgen receptor protein in spinal and bulbar muscular atrophy. Ann Neurol 44:249–254.

Li M, Nakagomi Y, Kobayashi Y, Merry DE, Tanaka F, Doyu M, Mitsuma T, Hashizume Y, Fischbeck KH, Sobue G (1998b) Nonneural nuclear inclusions of androgen receptor protein in spinal and bulbar muscular atrophy. Am J Pathol 153:695–701.

Li M, Chevalier-Larsen ES, Merry DE, Diamond MI (2007) Soluble androgen receptor oligomers underlie pathology in a mouse model of spinobulbar muscular atrophy. J Biol Chem 282:3157–3164.

Li P, Nijhawan D, Budihardjo I, Srinivasula SM, Ahmad M, Alnemri ES, Wang X (1997) Cytochrome c and dATP-dependent formation of Apaf-1/caspase-9 complex initiates an apoptotic protease cascade. Cell 91:479–489.

Lindholm D, Wootz H, Korhonen L (2006) ER stress and neurodegenerative diseases. Cell Death Differ 13:385–392.

Martinou JC, Dubois-Dauphin M, Staple JK, Rodriguez I, Frankowski H, Missotten M, Albertini P, Talabot D, Catsicas S, Pietra C, Huarte J (1994) Overexpression of BCL-2 in transgenic mice protects neurons from naturally occurring cell death and experimental ischemia. Neuron 13:1017–1030.

Mattson MP (2000) Apoptosis in neurodegenerative disorders. Nat Rev Mol Cell Biol 1:120–129.

Merry DE, Kobayashi Y, Bailey CK, Taye AA, Fischbeck KH (1998) Cleavage, aggregation and toxicity of the expanded androgen receptor in spinal and bulbar muscular atrophy. Hum Mol Genet 7:693–701.

Miyashita T, Okamura-Oho Y, Mito Y, Nagafuchi S, Yamada M (1997) Dentatorubral pallidoluysian atrophy (DRPLA) protein is cleaved by caspase-3 during apoptosis. J Biol Chem 272:29238–29242.

Morfini G, Pigino G, Szebenyi G, You Y, Pollema S, Brady ST (2006) JNK mediates pathogenic effects of polyglutamine-expanded androgen receptor on fast axonal transport. Nat Neurosci 9:907–916.

Moulder KL, Onodera O, Burke JR, Strittmatter WJ, Johnson EM Jr (1999) Generation of neuronal intranuclear inclusions by polyglutamine-GFP: analysis of inclusion clearance and toxicity as a function of polyglutamine length. J Neurosci 19:705–715.

Nakamura K, Jeong SY, Uchihara T, Anno M, Nagashima K, Nagashima T, Ikeda S, Tsuji S, Kanazawa I (2001) SCA17, a novel autosomal dominant

cerebellar ataxia caused by an expanded polyglutamine in TATA-binding protein. Hum Mol Genet 10:1441–1448.

Nishitoh H, Matsuzawa A, Tobiume K, Saegusa K, Takeda K, Inoue K, Hori S, Kakizuka A, Ichijo H (2002) ASK1 is essential for endoplasmic reticulum stress-induced neuronal cell death triggered by expanded polyglutamine repeats. Genes Dev 16:1345–1355.

Okada H, Mak TW (2004) Pathways of apoptotic and non-apoptotic death in tumour cells. Nat Rev Cancer 4:592–603.

Ona VO, Li M, Vonsattel JP, Andrews LJ, Khan SQ, Chung WM, Frey AS, Menon AS, Li XJ, Stieg PE, Yuan J, Penney JB, Young AB, Cha JH, Friedlander RM (1999) Inhibition of caspase-1 slows disease progression in a mouse model of Huntington's disease. Nature 399:263–267.

Pandey UB, Nie Z, Batlevi Y, McCray BA, Ritson GP, Nedelsky NB, Schwartz SL, DiProspero NA, Knight MA, Schuldiner O, Padmanabhan R, Hild M, Berry DL, Garza D, Hubbert CC, Yao TP, Baehrecke EH, Taylor JP (2007) HDAC6 rescues neurodegeneration and provides an essential link between autophagy and the UPS. Nature 447:859–863.

Paulson HL, Perez MK, Trottier Y, Trojanowski JQ, Subramony SH, Das SS, Vig P, Mandel JL, Fischbeck KH, Pittman RN (1997) Intranuclear inclusions of expanded polyglutamine protein in spinocerebellar ataxia type 3. Neuron 19:333–344.

Perrelet D, Ferri A, Liston P, Muzzin P, Korneluk RG, Kato AC (2002) IAPs are essential for GDNF-mediated neuroprotective effects in injured motor neurons in vivo. Nat Cell Biol 4:175–179.

Putcha GV, Moulder KL, Golden JP, Bouillet P, Adams JA, Strasser A, Johnson EM (2001) Induction of BIM, a proapoptotic BH3-only BCL-2 family member, is critical for neuronal apoptosis. Neuron 29:615–628.

Puthalakath H, O'Reilly LA, Gunn P, Lee L, Kelly PN, Huntington ND, Hughes PD, Michalak EM, McKimm-Breschkin J, Motoyama N, Gotoh T, Akira S, Bouillet P, Strasser A (2007) ER stress triggers apoptosis by activating BH3-only protein Bim. Cell 129:1337–1349.

Rao RV, Ellerby HM, Bredesen DE (2004) Coupling endoplasmic reticulum stress to the cell death program. Cell Death Differ 11:372–380.

Richter BW, Mir SS, Eiben LJ, Lewis J, Reffey SB, Frattini A, Tian L, Frank S, Youle RJ, Nelson DL, Notarangelo LD, Vezzoni P, Fearnhead HO, Duckett CS (2001) Molecular cloning of ILP-2, a novel member of the inhibitor of apoptosis protein family. Mol Cell Biol 21:4292–4301.

Saudou F, Finkbeiner S, Devys D, Greenberg ME (1998) Huntingtin acts in the nucleus to induce apoptosis but death does not correlate with the formation of intranuclear inclusions. Cell 95:55–66.

Schilling G, Becher MW, Sharp AH, Jinnah HA, Duan K, Kotzuk JA, Slunt HH, Ratovitski T, Cooper JK, Jenkins NA, Copeland NG, Price DL, Ross CA, Borchelt DR (1999a) Intranuclear inclusions and neuritic aggregates in transgenic mice expressing a mutant N-terminal fragment of huntingtin. Hum Mol Genet 8:397–407.

Schilling G, Wood JD, Duan K, Slunt HH, Gonzales V, Yamada M, Cooper JK, Margolis RL, Jenkins NA, Copeland NG, Takahashi H, Tsuji S, Price DL, Borchelt DR, Ross CA (1999b) Nuclear accumulation of truncated atrophin-1 fragments in a transgenic mouse model of DRPLA. Neuron 24:275–286.

Sekine Y, Takeda K, Ichijo H (2006) The ASK1-MAP kinase signaling in ER stress and neurodegenerative diseases. Curr Mol Med 6:87–97.

Sherman MY, Goldberg AL (2001) Cellular defenses against unfolded proteins: a cell biologist thinks about neurodegenerative diseases. Neuron 29:15–32.

Shinoe T, Wanaka A, Nikaido T, Kanazawa K, Shimizu J, Imaizumi K, Kanazawa I (2001) Upregulation of the pro-apoptotic BH3-only peptide harakiri in spinal neurons of amyotrophic lateral sclerosis patients. Neurosci Lett 313:153–157.

Skinner PJ, Koshy BT, Cummings CJ, Klement IA, Helin K, Servadio A, Zoghbi HY, Orr HT (1997) Ataxin-1 with an expanded glutamine tract alters nuclear matrix-associated structures. Nature 389:971–974.

Sopher BL, Thomas PS Jr, LaFevre-Bernt MA, Holm IE, Wilke SA, Ware CB, Jin LW, Libby RT, Ellerby LM, La Spada AR (2004) Androgen receptor YAC transgenic mice recapitulate SBMA motor neuronopathy and implicate VEGF164 in the motor neuron degeneration. Neuron 41:687–699.

Sperandio S, de Belle I, Bredesen DE (2000) An alternative, nonapoptotic form of programmed cell death. Proc Natl Acad Sci U S A 97:14376–14381.

Stennicke HR, Salvesen GS (1998) Properties of the caspases. Biochim Biophys Acta 1387:17–31.

Takeyama K, Ito S, Yamamoto A, Tanimoto H, Furutani T, Kanuka H, Miura M, Tabata T, Kato S (2002) Androgen-dependent neurodegeneration by polyglutamine-expanded human androgen receptor in *Drosophila*. Neuron 35:855–864.

Taylor JP, Hardy J, Fischbeck KH (2002) Toxic proteins in neurodegenerative disease. Science 296:1991–1995.

Taylor JP, Tanaka F, Robitschek J, Sandoval CM, Taye A, Markovic-Plese S, Fischbeck KH (2003) Aggresomes protect cells by enhancing the degradation of toxic polyglutamine-containing protein. Hum Mol Genet 12:749–757.

Turmaine M, Raza A, Mahal A, Mangiarini L, Bates GP, Davies SW (2000) Nonapoptotic neurodegeneration in a transgenic mouse model of Huntington's disease. Proc Natl Acad Sci U S A 97:8093–8097.

Urano F, Wang X, Bertolotti A, Zhang Y, Chung P, Harding HP, Ron D (2000) Coupling of stress in the ER to activation of JNK protein kinases by transmembrane protein kinase IRE1. Science 287:664–666.

Walcott JL, Merry DE (2002) Ligand promotes intranuclear inclusions in a novel cell model of spinal and bulbar muscular atrophy. J Biol Chem 277:50855–50859.

Wang HL, Yeh TH, Chou AH, Kuo YL, Luo LJ, He CY, Huang PC, Li AH (2006) Polyglutamine-expanded ataxin-7 activates mitochondrial apoptotic pathway of cerebellar neurons by upregulating Bax and downregulating Bcl-x(L). Cell Signal 18:541–552.

Warby SC, Doty CN, Graham RK, Carroll JB, Yang YZ, Singaraja RR, Overall CM, Hayden MR (2008) Activated caspase-6 and caspase-6-cleaved fragments of huntingtin specifically colocalize in the nucleus. Hum Mol Genet 17:2390–2404.

Wellington CL, Ellerby LM, Hackam AS, Margolis RL, Trifiro MA, Singaraja R, McCutcheon K, Salvesen GS, Propp SS, Bromm M, Rowland KJ, Zhang T, Rasper D, Roy S, Thornberry N, Pinsky L, Kakizuka A, Ross CA, Nicholson DW, Bredesen DE, Hayden MR (1998) Caspase cleavage of gene products associated with triplet expansion disorders generates truncated fragments containing the polyglutamine tract. J Biol Chem 273:9158–9167.

Whitfield J, Neame SJ, Paquet L, Bernard O, Ham J (2001) Dominant-negative c-Jun promotes neuronal survival by reducing BIM expression and inhibiting mitochondrial cytochrome c release. Neuron 29:629–643.

Willis SN, Fletcher JI, Kaufmann T, van Delft MF, Chen L, Czabotar PE, Ierino H, Lee EF, Fairlie WD, Bouillet P, Strasser A, Kluck RM, Adams JM, Huang DC (2007) Apoptosis initiated when BH3 ligands engage multiple Bcl-2 homologs, not Bax or Bak. Science 315:856–859.

Yuan J, Yankner BA (2000) Apoptosis in the nervous system. Nature 407:802–809.

Zoghbi HY, Orr HT (2000) Glutamine repeats and neurodegeneration. Annu Rev Neurosci 23:217–247.

Journal of the Neurological Sciences 279 (2009) 57–61

Contents lists available at ScienceDirect

Journal of the Neurological Sciences

journal homepage: www.elsevier.com/locate/jns

Intravenous immunoglobulin treatment for painful sensory neuropathy associated with Sjögren's syndrome

Saori Morozumi [a], Yuichi Kawagashira [a], Masahiro Iijima [a], Haruki Koike [a], Naoki Hattori [a], Masahisa Katsuno [a,b], Fumiaki Tanaka [a], Gen Sobue [a,*]

[a] Department of Neurology, Nagoya University Graduate School of Medicine, Japan
[b] Institsute for Advanced Research, Nagoya University, Nagoya, Japan

ARTICLE INFO

Article history:
Received 21 October 2008
Accepted 15 December 2008
Available online 24 January 2009

Keywords:
Sjögren's syndrome
Painful neuropathy
IVIg
VAS
Quantitative sensory testing (QST)
Sural nerve biopsy

ABSTRACT

Background: Patients with painful sensory neuropathy associated with Sjögren's syndrome-associated neuropathy often show severe neuropathic pain which is not relieved by conventional treatments.
Objective: To evaluate the effect of intravenous immunoglobulin (IVIg) therapy in the treatment of neuropathic pain associated with Sjögren's syndrome.
Patients and methods: We examined 5 patients affected by painful sensory neuropathy associated with Sjögren's syndrome. All patients were treated with IVIg (0.4 g/kg/day for 5 days) and pain rating was assessed by the Visual Analogue Scale (VAS).
Results: All five patients showed a remarkable improvement in neuropathic pain following IVIg therapy. Pain, assessed by the determination of mean VAS score, was reduced by 73.4% from days 2–14 following treatment. The observed clinical improvement persisted for 2 to 6 months. One patient, examined by quantitative sensory testing (QST), showed an improvement of superficial sensory deficit accompanied by pain relief.
Conclusion: IVIg might be an effective treatment for pain in Sjögren's syndrome-associated neuropathy. Further studies should be done in a controlled, blind study.

1. Introduction

Various forms of peripheral neuropathy have been reported to be associated with Sjögren's syndrome, including sensory ataxic neuropathy, painful sensory neuropathy without sensory ataxia, trigeminal neuropathy, multiple mononeuropathy, multiple cranial neuropathy, radiculoneuropathy, and autonomic neuropathy with anhidrosis [1–7]. The presence of such a diverse array of neuropathic states suggests that multiple mechanisms are involved in the pathogenesis of neuropathy associated with Sjögren's syndrome. Furthermore, the therapeutic efficacy of major treatments for Sjögren's syndrome, such as corticosteroid therapy, IVIg therapy and immunosuppressant therapy, appear to vary amongst the different forms of neuropathy [5], most probably reflecting differences in the underlying pathology. We previously reported, as an anecdotal case report, the effectiveness of IVIg therapy in the amelioration of painful symptoms of sensory neuropathy without the sensory ataxia associated with Sjögren's syndrome [8]. Pain in this type of neuropathy is often uncontrolled with conventional symptomatic treatment using NSAIDs, tricyclic antidepressant and anti-epileptic drugs, and can thus significantly compromise the activity of daily living [5]. Control of pain in the painful form of neuropathy without sensory ataxia is a major problem in Sjögren's syndrome-associated neuropathy, although this painful form is not widely recognized as a sub-form of Sjögren's syndrome-associated neuropathy [5].

In the present study, we evaluated the efficacy of IVIg therapy in five patients with painful sensory neuropathy associated with Sjögren's syndrome but without sensory ataxia and further characterize this type of neuropathy.

2. Patients and methods

We recruited five patients affected by the painful sensory neuropathy associated with Sjögren's syndrome. All five patients fulfilled the diagnostic criteria for Sjögren's syndrome. The diagnosis of primary Sjögren's syndrome was established by criteria proposed by the Diagnostic Committee of Health and Welfare of Japan [9] and by the American–European Community [10]. One of our patients (patient 1) has been described previously [8]. In the present study, we further present additional novel information regarding this patient, particularly in terms of long-term follow up and therapeutic outcome. Patients were excluded if they presented with other causes of neuropathy, including diabetes mellitus, impaired glucose tolerance, vitamin B12 deficiency, folic acid deficiency, autoimmune disease, and paraproteinemia. Hypothyroidism was evident in two patients (patients 4 and 5), although medication regulated thyroid function at

* Corresponding author. Department of Neurology, Nagoya University School of Medicine, Nagoya 466-8550 Japan. Tel.: +81 52 744 2385; fax: +81 52 744 2384.
E-mail address: sobueg@med.nagoya-u.ac.jp (G. Sobue).

0022-510X/$ – see front matter © 2008 Elsevier B.V. All rights reserved.
doi:10.1016/j.jns.2008.12.018

Table 1
Laboratory findings and clinical features

Patient age/sex	Dry eye/ dry mouth	Positive findings of Sjögren's syndrome	Initial symptom	Progression	Motor involvement		Sensory involvement					Autonomic involvement
					Weakness	Atrophy	Distribution	Superficial[a]	deep[b]	Spontaneous pain	Characteristics of pain	
1 67/M	-/-	SS-A, B lip biopsy	Pain	Chronic	–	–	L[c] (distal) T[c] (middle portion)	+	–	+++[d]	Aching hyperalgesia	1.2.3.4.5.6.
2 72/F	+/+	Lip biopsy	Pain	Chronic	–	–	L[c] (distal) H[c] (left side back)	+	–	+++[d]	Tingling hyperalgesia	1.2.4
3 54/M	+/+	SS-B lip biopsy	Sensory disturbance	Subacute	–	–	Right hand (radial) L[c] (dital) T[c] (upper portion)	+	–	+++[d]	Tingling static allodynia hyperalgesia	–
4 57/F	+/+	SS-A lip biopsy	Pain	Subacute	–	–	L[c] (distal)	–	–	+/+	Aching hyperalgesia	2.4
5 59/F	+/–	SS-A lip biopsy	Pain	Chronic	+	–	F[c] (left side) L[c] (upper) L[c] (right>left)	+	+	+++[d]	Tingling hyperalgesia	2.3.4

1, Abnormal pupils; 2, Hypohidrosis; 3, Orthostatic hypotension; 4, Constipation; 5, Urinary disturbance; 6, Decreased uptake of ^{123}I-MIBG.
[a] Superficial; reduction of superficial sensation including light touch and pinprick perception and temperature sensation.
[b] Deep; reduction of deep sensation including vibration and joint position.
[c] F, Face; H, Head; L, Limb; T, Trunk.
[d] 'Å{Å{, moderate pain; 'Å{Å{Å{, severe pain.

normal levels in these patients. Prior to treatment, all patients underwent neurological examination, blood studies, CSF studies, nerve conduction studies (NCS), and sural nerve biopsy. Profiles of the patients are summarized in Tables 1, 2, and 3. The group of patients included two men and three women, ranging from 54 to 72 years old. In all patients, the initial symptom of neuropathy was paraesthesia or painful peripheral dysaesthesia in the distal portion of the extremities.

Patient 1, a 67 year old man, was diagnosed as Sjögren's syndrome 16 years ago, had suffered painful dysaesthesia and numbness in the feet for 10 years, which spread to the proximal portion of the legs and arms. Neurological examination revealed a reduction in superficial sensation, including light touch/pinprick perception and temperature sensation; painful dysaesthesias were elicited over the middle portion of the trunk and the four extremities. The pain experienced in this patient's hands was so intense that he could not extend his fingers or touch objects. The pain in his feet almost precluded ambulation. *Patient 2*, a 72 year old woman had experienced painful dysaesthesia and numbness in the legs and hands for 3 years. Neurological examination revealed reduced superficial sensation along with painful dysaesthesias in the distal portion of the four extremities. *Patient 3*, a 54 year old man, had experienced pain in all four extremities and the head for 4 years. Neurological examination revealed no reduction in superficial sensation. Hyperalgesia was evident over the left side of the back of the head, the upper portion of the trunk, and the radial side of the right hand and feet. The patient needed to wear gloves to protect himself from the hand pain during his normal daily life. Sometimes, the patient also experienced difficulty walking as a direct result of pain. *Patient 4*, a 57 year old woman had suffered pain in her left foot for 1 year. Neurological examination revealed a reduction in superficial sensation; painful dysaesthesias were elicited over distal parts of the four extremities. *Patient 5*, a 59 year old woman had suffered spontaneous pain for 20 years along with painful dysaesthesia and numbness in all four extremities, but predominantly on the right side. Neurological examination revealed reduced superficial sensation. Painful dysaesthesias were elicited over the left-side cheek, the radial side of the upper extremities, and the lower extremities, predominantly on the right side. The pain in this patient's legs almost precluded ambulation.

Fluctuation in the intensity of pain was seen, to some extent, in all patients. Asymmetric pain symptoms and sensory impairments were seen in three patients (patients 3, 4, and 5). Although deep sensation, such as joint position and vibration, was mildly impaired in the distal portion of the extremities in one patient (patient 5), this was not accompanied by sensory ataxia, pseudoathetosis in the hand, or a

Table 2
Nerve conduction study

Patient	Median nerve					Tibial nerve			Sural nerve	
	MCV (m/s)	DL (ms)	CMAP (mV)	SCV (m/s)	SNAP (μV)	MCV (m/s)	DL (ms)	CMAP (mV)	SCV (m/s)	SNAP (μV)
1	56	3.4	5.4	48	5.2	42	4.2	7.1	47	3.9
2	55	3.1	4.5	64	23	32	4.1	5.7	43	17
3	55	3.1	12.6	63	25.1	48	3.9	15.8	51	27.2
4	54	2.9	10.3	58	41.6	40	4.6	10.5	60	15.5
5	55	2.7	6.1	62	25.2	42	3.4	15.9	48	11.5
Controls	57.6±3.8	3.4±0.4	8.2±2.9	56.3±5.3	28.0±11.5	46.0±3.8	4.0±0.6	11.8±3.5	49.2±4.8	16.8±7.8

Control values were obtained in 171 normal volunteers for the median nerve, 161 for the ulnar nerve, and 163 for the sural nerve [11].
MCV = motor nerve conduction velocity; DL = distal latency; CMAP = compound muscle action potential.
SCV = sensory nerve conduction velocity; SNAP = sensory nerve action potential.

Table 3
Pathological findings in the sural nerve

Patient	Myelinated fiber density (no/mm^2)			Small/large ratio	Unmyelinated fiber density (no/mm^2)	Tested-fiber study (%)	
	Total fiber	Large fiber	Small fiber			De/re-myelination	Axonal degeneration
1	4557	1778	2779	1.6	19,245	3.0	24.0
2	5728	2594	3134	1.2	13,557	8.0	0.3
3	6085	2845	3240	1.1	17,118	0.5	0.5
4	6902	3530	3372	1.0	13,397	1.1	1.9
5	4807	2766	2041	0.7	21,531	6.2	2.8
Controls (n=10) mean±SD	7087±1413	2717±617	4363±1067	1.7±0.5	30,876±3713	9.0±5.9	1.8±2.0

Control values were obtained from subjects with nonneurologic disease at autopsy.

positive Romberg's sign. Muscle strength was preserved in all patients except for patient 5; this particular patient could not exert full muscle strength in the right lower extremity due to severe pain, and appeared to reveal slight weakness. Autonomic dysfunctions, including constipation, orthostatic hypotension and hypohidrosis were seen in four of the patients. Reduced uptake of ^{123}I-MIBG was evident in two patients (Table 1). Cerebrospinal fluid cell count was normal in all patients, while protein was elevated in two patients (patients 1 and 5). Nerve conduction studies revealed preserved motor and sensory conduction velocities and distal latencies (Table 2). Amplitudes of compound muscle action potential (CMAP) and sensory nerve action potential (SNAP) were greater than the mean±2SD of normal control subjects [11], except for SNAP of the median nerve in patient 1. Sural nerve specimens revealed mild reduction in small-myelinated fibers and unmyelinated fibers in all patients (Fig. 1, Table 3). The density of large myelinated fibers was 2720±627 fibers/mm^2 (100% of mean control values), while that of small myelinated fibers was 2913±535 fibers/mm^2 (66% of mean control values), indicating a predominant reduction in the number of small myelinated fibers. The density of unmyelinated fiber was 16,970±3550 fibers/mm^2 (55% of mean control values). Axonal degeneration was evident in patient 1. There was no evidence of axonal sprouting in any of the patients, suggesting ganglionopathy as a cause of neuropathy. Vasculitis was not observed in any patient.

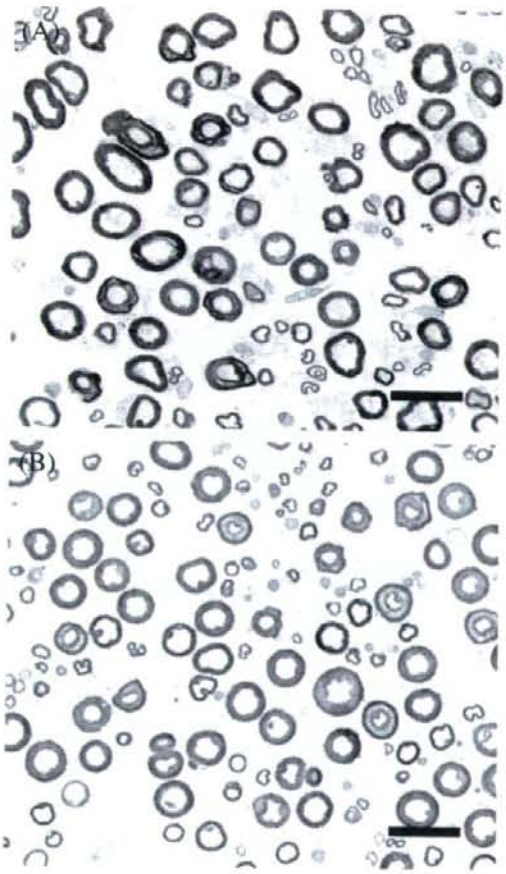

Fig. 1. Sural nerve pathology. (A) Specimen from patient 4. (B) Specimen from a control patient. Specimen from patient 4 revealed predominantly small-fiber loss. No axonal sprouting was seen. Vasculitis was not observed. Scale bar=20 μm.

All patients were treated with 0.4 g/kg intravenous immunoglobulin (IVIg) for 5 days. In all patients, the effect of IVIg treatment was scored by use of the Visual Analogue Scale (VAS) [12]. In addition, we performed quantitative sensory testing (QST) to determine the cold detection threshold (CDT), vibration detection threshold (VDT), and heat-pain (HP) threshold in both the upper and lower extremities using computer aided sensory evaluation version (CASE : Medical Electronics, Michigan). This evaluation was carried out on one patient (patient 5), before and after treatment. For the CDT, a series of cold stimulation tests, using a range of different temperatures were delivered with a sensor placed on the dorsum of the foot. Patients were asked to respond when the stimulus was felt. The testing algorithms used were the 4, 2, and 1 stepping method for CDT [13], the aim being to determine the smallest temperature differential from the baseline temperature that can be reliably detected. For the VDT, a series of vibration stimulation tests were delivered with a sensor placed on the great toe using the 4, 2, and 1 stepping method. For the HP thresholds, a series of warm stimulation tests were delivered to the dorsum of the foot, using the non-repeating ascending with null stimuli algorithm [14]. HP: 0.5 is the heat-pain detection threshold, HP: 5.0 is a intermediate heat-pain response and the difference between the two (HP: 5.0−0.5). CASE IV normative data were used in accordance with previous studies [13]. Abnormal CDT and VDT were defined as above the 97th percentile (hypoesthesia), and an abnormal HP: 0.5 was defined as below the 3rd percentile (hyperalgesia). QST studies were performed by the same technician in two different patients (patients 4 and 5).

3. Results

All patients responded well to IVIg therapy. Severe pain had been reduced from 7.6±2.9 to 2.2±1.5, according to the Visual Analogue Scale (VAS) (Fig. 2). Several relapses were seen in two patients (patients 1 and 2) over long-term follow up. IVIg treatment was effective at each relapse, but the effect of IVIg became less pronounced in patient 2 after 6 years of treatment (Fig. 2 B). The effect on pain was reported to begin 2 to 14 days after the IVIg infusion started. The clinical improvement lasted for about 2 to 6 months (4.0±2.65 months). The second IVIg therapies were performed in four patients when relapse occurred, with the interval of second IVIg

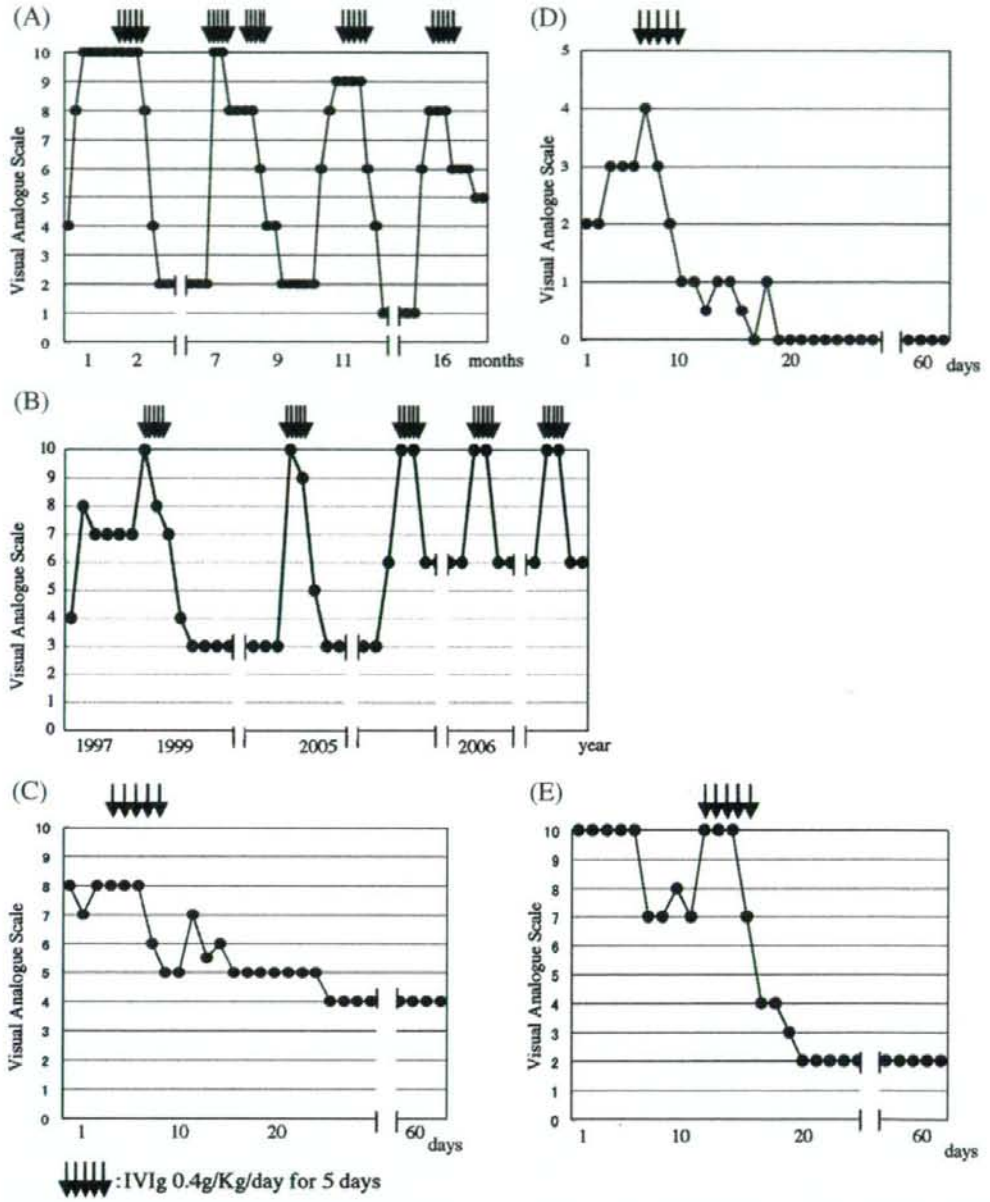

Fig. 2. Clinical course of the Visual Analogue Scale. A 10 cm VAS was anchored by two extremes of pain (left, no pain; right, the worst pain imaginable). Pain ratings were applied subjectively according to the manner described by Kelly [12]. (A) Clinical course of patient 1. (B) Clinical course of patient 2. (C) Clinical course of patient 3. (D) Clinical course of patient 4. (E) Clinical course of patient 5.

treatment ranging from 7 months to 1 year. IVIg therapy reduced pain by 50–100% on the VAS scale; the significant effect of IVIg upon pain relief was clearly evident ($p<0.01$). All patients experienced accompanied superficial sensation, such as numbness, tingling or painful dysaesthesia, but these showed simultaneous improvement. Muscle strength in patient 5 also improved. Following IVIg treatment, patients 1, 3 and 5 were able to walk smoothly and patient 3 no longer required gloves. Direct evidence of sensory improvement was clearly demonstrated by CASE IV analysis in patient 5. VDT 5 was less than +2SD and there was no significant difference before and after treatment. Before treatment, CDT was 28.1 °C (hand) and 10.0 °C (foot), representing abnormal levels greater than +2SD. Following IVIg therapy, CDT improved to 29.8 °C (hand) and 17.3 °C (foot), which was within the normal range of −1.04SD (hand) and +1.88SD (foot). These results clearly demonstrate significant improvement in superficial sensory impairment following IVIg therapy. HP threshold was not different before and after treatment.

4. Discussion

IVIg therapy was effective in alleviating pain symptoms in all 5 patients involved in the present study. Painful symptoms involved

proximal regions of the limbs, face, or trunk in a non-length dependent manner with predominantly superficial sensory involvement. Motor nerve function was well preserved. Pathologically, there was a predominantly small-fiber axon loss with relative preservation of large myelinated axons, without evidence of regenerating fibers. Pathological evaluation of the dorsal root ganglia in patients with major causes of ganglionopathy have been reported for patients with Sjögren's syndrome and paraneoplastic syndrome, via the analysis of tissue obtained by biopsy or autopsy [2,15]. The major symptom in these syndromes is sensory ataxia resulting from the impairment of deep kinaesthetic sensation corresponding to the involvement of large-sized neurons [2,15]. On the other hand, it is uncommon for ganglionopathy to preferentially affect small-diameter neurons [16,17]. However, recent studies have suggested that this type of ganglionopathy may occur in patients with Sjögren's syndrome accompanying painful symptoms [5,17]. Our patients were well concordant with these clinico-pathological features of ganglionopathy with preferential involvement of small-sensory neurons. The concept of ganglionopathy, preferentially involving small neurons, although not yet widely recognized, is rapidly becoming a clinically important field [17].

In our patients, painful symptoms were very severe and significantly interfered with the activity of daily living. Conventional treatments for painful neuropathies, including anticonvulsants, tricyclic antidepressants, SSRI (selective serotonin reuptake inhibitor) or opioids, were not sufficient to ameliorate pain in our patients. Consequently, it was highly evident that other new approaches were needed. Although the mechanisms of pain in painful sensory neuropathy associated with Sjögren's syndrome have yet to be fully clarified, it is considered that immunomodulatory therapy may be effective, based on the hypothesis that painful sensory neuropathy is a continuum of the sensory ataxic form as described above. In the sensory ataxic form, the lesion is located at the level of the sensory ganglion neurons associated with T-cell infiltration [2]. Indeed, IVIg therapy has proved to be effective, to some extent, in the sensory ataxic form [5,18–21]. The putative IVIg effect mechanism includes blockade of the Fc receptor, enhanced antibody catabolism and the suppression of pro-inflammatory cytokines. Therefore, macrophage and B-cell functions would be inactivated and circulating auto-antibodies reduced. IVIg can also exert effect upon superantigens and can modulate T-cell function and antigen recognition [22]. In the ataxic type of Sjögren's syndrome, some of the remaining dorsal root ganglion neurons, which tend to be impaired owing to inflammation, may have regained function because of the IVIg treatment [21]. We speculate that IVIg would elicit the same effect upon small dorsal root ganglion neurons in painful Sjögren's syndrome-neuropathy.

Pro-inflammatory cytokines such as TNF-alpha, IL-1 beta, and IL-6 contribute to the development of inflammatory and neuropathic pain, and hyperalgesia [23,24]. Indeed, in patients with painful neuropathy, or complex regional pain syndrome, TNF-alpha has been reported to correlate with the presence of mechanical hyperalgesia [25,26]. However, participation of such cytokines in painful sensory neuropathy associated with Sjögren's syndrome remains largely unknown. In one of our patients, some serum cytokines, e.g., TNF-α, IL-8 were shown to be reduced by IVIg (patient 3, data not shown). A question of IVIg treatment is cost. It is certain that IVIg is very expensive, but IVIg bring rapid and sufficient improvement. Therefore, IVIg treatment is considered to be useful for patients who have severe pain or have insufficient improvement by conventional treatment. Therefore, IVIg might be an effective treatment for pain in Sjögren's syndrome-associated neuropathy. Further studies should be done in a controlled, blind study.

References

[1] Grant IA, Hunder GG, Homburger HA, Dyck PJ. Peripheral neuropathy associated with sicca complex. Neurology 1997;48:855–62.
[2] Griffin JW, Cornblath DR, Alexander E, Champbell J, Low PA, Bird S, et al. Ataxic sensory neuropathy and dorsal root ganglionitis associated with Sjögren's syndrome. Ann Neurol 1990;27:304–15.
[3] Kaltreider HB, Talal N. The neuropathy of Sjögren's syndrome. Trigeminal nerve involvement. Ann Intern Med 1969;70:751–62.
[4] Kumazawa K, Sobue G, Yamamomto K, Mitsuma T. Segmental anhidrosis in the spinal dermatomes in Sjögren's syndrome-associated neuropathy. Neurology 1993;43:1820–3.
[5] Mori K, Iijima M, Koike H, Hattori N, Tanaka F, Watanabe H, et al. The wide spectrum of clinical manifestations in Sjogren's syndrome-associated neuropathy. Brain 2005;128:2518–34.
[6] Peyronnard JM, Charron L, Beaudert F, Couture F. Vasculitic neuropathy in rheumatoid disease and Sjögren syndrome. Neurology 1982;32:839–45.
[7] Sobue G, Yasuda T, Kachi T, Sakakibara T, Mitsuma T. Chronic progressive sensory ataxic neuropathy: clinicopathological features of idiopathic and Sjögren's syndrome-associated cases. J Neurol 1993;240:1–7.
[8] Kizawa M, Mori K, Iijima M, Koike H, Hattori N, Sobue G. Intravenous immunoglobulin treatment in painful sensory neuropathy without sensory ataxia associated with Sjögren's syndrome. J Neurol Neurosurg Psychiatry 2006;77:967–9.
[9] Fujibayashi T, Sugai S. Revised Japanese diagnostic criteria for Sjögren's syndrome. Annual Report of Research Committee for Immune Disease. Tokyo: Japanese Ministry of Health and Welfare; 1999. p. 35–8.
[10] Vitali C, Bombardieri S, Jonsson R, Moutsopoulos HM, Alexander EL, Carsons SE, et al. Classification criteria for Sjögren's syndrome: a revised version of the European criteria proposed by the American–European Consensus Group. Ann Rheum Dis 2002;61:554–8.
[11] Koike H, Hirayama M, Yamamoto M, Ito H, Hattori N, Umehara F, et al. Age associated axonal features in HNPP with 17p11.2 deletion in Japan. J Neurol Neurosurg Psychiatry 2005;76:1109–14.
[12] Kelly AM. The minimum clinically significant difference in visual analogue scale pain score dose not differ with severity of pain. Emerg Med J 2001;18:205–7.
[13] Dyck PJ, O'Brien PC, Kosanke JL, Gillen DA, Karnes JL. A 4, 2, and 1 stepping algorithm for quick and accurate estimation of cutaneous sensation threshold. Neurology 1993;43:1508–12.
[14] Dyck PJ, Zimmerman IR, Johnson DM, Gillen D, Hokanson JL, Karnes JL, et al. A standard test of heat-pain responses using CASE IV. J Neurol Sci 1996;136:54–63.
[15] Ohnishi A, Ogawa M. Preferential loss of large lumbar primary sensory neurons in carcinomatous sensory neuropathy. Ann Neurol 1986;20:102–4.
[16] Gorson KC, Herrmann DN, Thiagarajan R, Braaga TH, Chi RL, Kinsella LJ, et al. Non-length dependent small fibre neuropathy/ganglionopathy. J Neurol Neurosurg Psychiatry 2008;79:113.
[17] Koike H, Sobue G. Small neurons may be preferentially affected in ganglionopathy. J Neurol Neurosurg Psychiatry 2008;79:113.
[18] Donofrio PD. Immunotherapy of idiopathic inflammatory neuropathies. Muscle Nerve 2003;28:273–92.
[19] Levy Y, Uziel Y, Zandman GG, Amital H, Sherer Y, Langevitz P, et al. Intravenous immunoglobulins in peripheral neuropathy associated with vasculitis. Ann Rheum Dis 2003;62:1221–3.
[20] Molina JA, Benito-Leon J, Bermejo F, Jiménez-Jiménez FJ, Oliván J. Intravenous immunoglobulin therapy in sensory neuropathy associated Sjögren's syndrome. J Neurol Neurosurg Psychiatry 1996;60:699.
[21] Takahashi Y, Takata T, Hosino M, Sakurai M, Kanawaza I. Benefit of IVIG for long-standing ataxic sensory neuronopathy with Sjögren's syndrome. IV immunoglobulin. Neurology 2003;60:503–5.
[22] Dalakas MC. Mechanism of action of intravenous immunoglobulin and therapeutic considerations in the treatment of autoimmune neurologic diseases. Neurology 1998;51:S2–8.
[23] Milligan ED, Twining C, Chacur M, Biedenkapp J, O'Connor K, Poole S, et al. Spinal glia and proinflammatory cytokines mediate mirror-image neuropathic pain in rats. J Neurosci 2003;23:1026–40.
[24] Opree A, Kress M. Involvement of the proinflammatory cytokines tumor necrosis factor-alpha, IL-1 beta, and IL-6 but not IL-8 in the development of heat hyperalgesia: effects on heat-evoked calcitonin gene-related peptide release from rat skin. J Neurosci 2000;20:6289–93.
[25] Empl M, Renaud S, Erne B, Fuhr P, Straube A, Schaeren-Wiemers N, et al. TNF-alpha expression in painful and nonpainful neuropathies. Neurology 2001;56:1371–7.
[26] Maihofner C, Handwerker HO, Neundörfer B, Birklein F. Mechanical hyperalgesia in complex regional pain syndrome: a role for TNF-alpha? Neurology 2005;65:311–3.

Phase 2 Trial of Leuprorelin in Patients with Spinal and Bulbar Muscular Atrophy

Haruhiko Banno, MD, PhD,[1] Masahisa Katsuno, MD, PhD,[1,2] Keisuke Suzuki, MD, PhD,[1] Yu Takeuchi, MD,[1] Motoshi Kawashima, MD,[1] Noriaki Suga, MD,[1] Motoko Takamori, MD, PhD,[3] Mizuki Ito, MD, PhD,[1] Tomohiko Nakamura, MD, PhD,[1] Koji Matsuo, MD, PhD,[1] Shinichi Yamada, MD, PhD,[1] Yumiko Oki, MD, PhD,[4] Hiroaki Adachi, MD, PhD,[1] Makoto Minamiyama, MD, PhD,[1] Masahiro Waza, MD, PhD,[1] Naoki Atsuta, MD, PhD,[1] Hirohisa Watanabe, MD, PhD,[1] Yasushi Fujimoto, MD, PhD,[5] Tsutomu Nakashima, MD, PhD,[5] Fumiaki Tanaka, MD, PhD,[1] Manabu Doyu, MD, PhD,[6] and Gen Sobue, MD, PhD[1]

Objective: Spinal and bulbar muscular atrophy (SBMA) is a hereditary motor neuron disease caused by the expansion of a polyglutamine tract in the androgen receptor (AR). Animal studies have shown that the pathogenesis of SBMA is dependent on serum testosterone level. This study is aimed at evaluating the efficacy and safety of androgen deprivation by leuprorelin acetate in patients with SBMA.

Methods: Fifty SBMA patients underwent subcutaneous injections of leuprorelin acetate or placebo in a randomized, placebo-controlled trial for 48 weeks, followed by an open-label trial for an additional 96 weeks, in which 19 patients of the leuprorelin group and 15 of the placebo group received leuprorelin acetate. The patients who did not participate in the open-label trial were also followed up for the 96-week period (UMIN000000474).

Results: Leuprorelin acetate significantly extended the duration of cricopharyngeal opening in videofluorography and decreased mutant AR accumulation in scrotal skin biopsy. The patients treated with leuprorelin acetate for 144 weeks exhibited significantly greater functional scores and better swallowing parameters than those who received placebo. Autopsy of one patient who received leuprorelin acetate for 118 weeks suggested that androgen deprivation inhibits the nuclear accumulation or stabilization, or both, of mutant AR in the motor neurons of the spinal cord and brainstem.

Interpretation: These observations suggest that administration of leuprorelin acetate suppresses the deterioration of neuromuscular impairment in SBMA by inhibiting the toxic accumulation of mutant AR. The results of this phase 2 trial support the start of large-scale clinical trials of androgen deprivation for SBMA.

Ann Neurol 2009;65:140–150

Spinal and bulbar muscular atrophy (SBMA), also known as Kennedy's disease, is the first of the neurodegenerative diseases for which the molecular basis was discovered to be the expansion of a trinucleotide CAG repeat in the gene of the causative protein. SBMA is an adult-onset, motor neuron disease characterized by muscle atrophy, weakness, contraction fasciculations, and bulbar involvement.[1–4] Its prevalence has been estimated to be 1 to 2 per 100,000, although a considerable number of patients may be misdiagnosed with other neuromuscular diseases such as amyotrophic lateral sclerosis (ALS).[5,6] The progression of SBMA is usually slow, but life-threatening respiratory tract infections often occur in the advanced stage of the disease, resulting in death.[7] Laboratory tests show increased serum levels of creatine kinase and liver enzymes in most cases. The expanded CAG triplet repeat sequence, which encodes a polyglutamine tract, is found in the androgen receptor gene *(AR)*.[8] The CAG repeat numbers range from 38 to 62 in SBMA patients, whereas healthy individuals have 9 to 36 CAGs.[5,8–10] The number of CAGs is correlated with disease severity and inversely correlated with the age of onset, as observed in other polyglutamine-related neurodegenerative dis-

From the [1]Department of Neurology, Nagoya University Graduate School of Medicine; [2]Institute for Advanced Research, Nagoya University, Nagoya; [3]Department of Neurology, Shizuoka Saiseikai General Hospital, Shizuoka; [4]Department of Neurology, Aichi Saiseikai Hospital; [5]Department of Otorhinolaryngology, Nagoya University Graduate School of Medicine, Nagoya; and [6]Department of Neurology, Aichi Medical University, Aichi, Japan.

Address correspondence to Dr Sobue and Dr. Katsuno, Department of Neurology, Nagoya University Graduate School of Medicine, 65 Tsurumai-cho, Showa-ku, Nagoya 466-8550, Japan.
E-mail: sobueg@med.nagoya-u.ac.jp; ka2no@med.nagoya-u.ac.jp

Potential conflict of interest: Nothing to report.

Additional Supporting Information may be found in the online version of this article.

Received Jul 15, 2008, and in revised form Aug 25. Accepted for publication Sep 5, 2008.

Published online in Wiley InterScience (www.interscience.wiley.com). DOI: 10.1002/ana.21540

eases, including Huntington's disease and several forms of spinocerebellar ataxia.[11,12] In polyglutamine diseases, nuclear localization of the respective mutant protein is considered important for inducing neuronal cell dysfunction and degeneration.[13–15] The extent of diffuse nuclear accumulation of mutant AR in spinal motor neurons is closely related to the CAG repeat length in autopsied SBMA cases.[16] In addition, nuclear accumulation of mutant AR in scrotal skin correlates with both disease severity and CAG repeat length, suggesting that the number of scrotal skin epithelial cells positive for 1C2, an anti-polyglutamine antibody, is a potent pathogenic marker of SBMA and can serve as a useful biomarker in therapeutic trials.[17]

A characteristic clinical feature of SBMA is that full disease manifestations occur in male but not in female individuals even when they are homozygous for the mutation.[18,19] The sex dependency of disease manifestation in SBMA may arise from a testosterone-dependent nuclear accumulation of mutant AR.[20–23] In mouse models of SBMA, surgical castration delays disease onset and progression, as well as reverses neuromuscular phenotypes.[20,23] Leuprorelin acetate, a luteinizing hormone–releasing hormone agonist that reduces testosterone release from the testis and inhibits nuclear accumulation of mutant AR, ameliorates motor dysfunction in male transgenic mice carrying full-length mutant human *AR* with an expanded polyglutamine tract.[21]

Although data from animal studies indicated that androgen deprivation via leuprorelin acetate is a promising therapeutic agent for SBMA,[20,21] clinical experience using this drug in SBMA patients is limited.[24] The safety and efficacy of leuprorelin acetate were demonstrated for treating prostate cancer, endometriosis, uterine fibroids, and central precocious puberty in children.[25] To determine whether androgen deprivation therapy prevents the progression of SBMA in humans, we conducted a two-arm, randomized, placebo-controlled, phase 2 clinical trial of leuprorelin acetate in patients with SBMA for 48 weeks, followed by an open-label trial for an additional 96 weeks.

Patients and Methods

Patients

Inclusion criteria of this trial included: (1) genetically confirmed SBMA male Japanese patients with more than one of the following symptoms: muscle weakness, muscle atrophy, bulbar palsy, or hand tremor; (2) patients whose *AR* CAG repeat length was more than 38; (3) patients who were 30 to 70 years old at the time of informed consent; (4) patients who had no desire to father a child; and (5) patients who gave written informed consent. Patients were excluded if they met any of the following criteria: (1) medical history of allergy to leuprorelin acetate; (2) had taken testosterone within 8 weeks before the informed consent; (3) had severe complications; or (4) were not eligible for other reasons (eg, previous use of luteinizing hormone–releasing hormone agonists or medical history of allergy to barium sulfate).

Study Design

We conducted a 48-week, prospective, randomized, placebo-controlled, single-site trial and a 96-week open-label follow-up trial at Nagoya University Hospital (Fig 1). Fifty patients were included between September 2003 and March 2004. The last patient terminated the randomized controlled trial (RCT) in February 2005. The protocol for the trial was filed with the open clinical trial registry (www.umin.ac.jp/ctr/index.htm) under the Identifier Number UMIN000000474. In the 48-week RCT, patients were randomized in a 1:1 ratio of leuprorelin acetate or identically appearing placebo using the minimization method by an independent investigator. Dynamic allocation was performed based on patient age and severity to reduce bias.[26] Patients were blinded throughout the RCT, and at week 48, they decided whether to participate in the follow-up trial without knowing to which drug group they had been allocated. As a result, 19 patients in the leuprorelin group and 15 in the placebo group entered the open-label follow-up trial between August 2004 and March 2005. The remaining 15 patients who declined to participate in the open-label trial were followed up for these 96 weeks; 1 patient who discontinued early in the 48-week RCT was not followed up. The last patient terminated the follow-up trial in February 2007.

All the examinations and treatments were performed at the Nagoya University Hospital throughout the trials. The patients were hospitalized for 7 days at weeks 0 and 48, and were evaluated every 4 weeks in the 48-week RCT. During the 96-week follow-up trial, they were examined every 12 weeks. Blinding was ensured by the use of identical opaque injection syringes. Clinical scores and muscle strength were assessed by blinded neurologists throughout the RCT period.

Treatment

Leuprorelin acetate was subcutaneously injected at a dose of 3.75mg every 4 weeks in the 48-week RCT, and 11.25mg was administrated every 12 weeks in the 96-week follow-up trial. Leuprorelin acetate suppresses testosterone release by downregulating luteinizing hormone–releasing hormone receptors in the pituitary. We did not conduct a dose–response study in this trial, because previous studies suggested that leuprorelin-mediated androgen deprivation is incomplete at dosages less than 3.75mg/4 weeks in men.[27,28]

Outcome Measures

The primary end point of this trial was motor function measured by the widely used and validated Revised ALS Functional Rating Scale (ALSFRS-R; Japanese edition). Although there are no validated scales for SBMA, all the items in the ALSFRS-R are applicable to this disease.[17,29,30] Secondary outcome measures included cricopharyngeal opening duration visualized by videofluorography (VF), the frequency of 1C2-positive cells in scrotal skin biopsies, lung function values [forced expiratory volume in 1 second/forced vital capacity (FEV_1/FVC) and vital capacity as the percentage of pre-

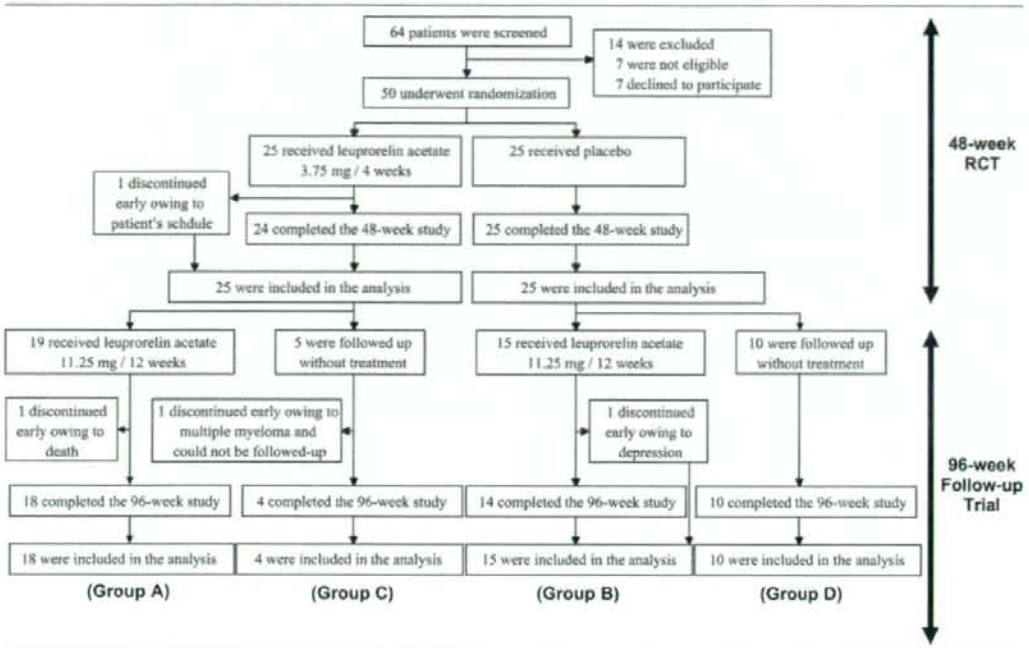

Fig 1. Patient selection flow diagram. RCT = randomized controlled trial.

dicted (%VC)], and serum levels of the following enzymes: L-aspartate aminotransferase, L-alanine aminotransferase, and creatine kinase. As other outcome measures, we analyzed the sum of the following three ALSFRS-R subscores: speech, salivation, and swallowing. We also measured muscle strength using maximum voluntary isometric contraction and conducted a nerve conduction study. The Beck depression inventory and standard laboratory parameters were checked for evaluating safety. Scrotal skin biopsies were performed at weeks 0 and 48 of the 48-week RCT. The ALSFRS-R, lung function test, maximum voluntary isometric contraction, and Beck depression inventory were measured every 24 weeks throughout the trials, whereas VF was examined at weeks 0 and 48 in the 48-week RCT, and at the end of the 96-week follow-up trial. The nerve conduction study was conducted at weeks 0 and 48 in the 48-week RCT. All laboratory tests were performed at weeks 0, 4, 8, 12, 24, 36, and 48 in the 48-week RCT, and every 12 weeks in the 96-week follow-up trial. Outcome for the efficacy analysis was assessed at the final visit at the end of 48-week RCT and at the end of the 96-week follow-up trial.

In VF examinations, patients were instructed to swallow 3ml of 40% wt/vol barium sulfate twice in a standing position. VF data were recorded on Mini DV videotape (Sony, Tokyo, Japan) at 30 frames/sec. For scrotal skin biopsies at 0 and 48 weeks, three specimens were taken from each patient at each time by punch biopsy using a 3mm diameter Dermapunch (Nipro, Tokyo, Japan) under local anesthesia (lidocaine acetate, 10ml) and processed for immunohistochemical analysis using an anti-polyglutamine (1C2) antibody, as described later. All 50 patients underwent biopsies at week 0, but 2 patients' specimens did not attach to the slides and were not included in the analyses. All patients who underwent biopsy sterilized the wound for several days themselves and underwent antibiotic therapy after the procedure, as needed. Serum creatine kinase levels were determined in blood samples obtained on the second day of admission by ultraviolet measurement using hexokinase and glucose-6-phosphate.[31] Serum testosterone levels were measured by radioimmunoassay using the DPC total testosterone kit (Diagnostic Products Corporation, Los Angeles, CA).

Quantitative Measurement in Videofluorography

To identify the appropriate parameters for the outcome measure in this trial, we performed a preliminary analysis of quantitative swallowing evaluation using VF in 18 additional SBMA patients (see Supplemental Tables 1 and 2). In this preliminary study, we assessed the reliability and validity of pharyngeal residue and those of the various temporal measures: pharyngeal delay time, cricopharyngeal opening duration, and total duration of maximal laryngeal elevation. As a result, we found that cricopharyngeal opening duration was the most reliable measurement of swallowing, and that this duration correlated well with functional scores such as the Norris Scores and the ALSFRS-R. None of the other parameters exhibited both high reliability and correlation with functional scores. Therefore, we adopted cricopharyngeal

opening duration as the secondary end point of this trial and measured other parameters as references. All the parameters were measured blindly by two independent evaluators according to standard procedures.[32,33] In brief, duration of cricopharyngeal opening was defined as the length of time during which the cricopharyngeal sphincter was open. Pharyngeal delay time was defined as the interval from the bolus passing the base of the tongue to the onset of laryngeal elevation, whereas duration of maximum laryngeal elevation was the length of time during which the larynx was maximally elevated from its rest position. Pharyngeal residue was measured using semiquantitative scales: 0, 2, 5, 10, 20, 30, 40, 50, 60, 70, 80, 90, and 100%.

Immunohistochemical Detection of Mutant Androgen Receptor

Immunohistochemistry of scrotal skin (from biopsies), spinal cord, and pontine base (from autopsies) specimens were conducted as described previously.[16,17] In brief, 6μm-thick, formalin-fixed, paraffin-embedded sections were prepared, deparaffinized, rehydrated, and pretreated by immersing in 98% formic acid for 5 minutes and then microwaving for 15 minutes in 10mM citrate buffer at pH 6.0. Sections were incubated with a mouse antiexpanded polyglutamine antibody (1C2; 1:20,000; Chemicon, Temecula, CA)[34] to evaluate the nuclear accumulation of mutant AR.[16,20,21] Immune complexes were visualized using the Envision-plus kit (Dako, Glostrup, Denmark). Sections were counterstained with Mayer's hematoxylin. Quantitative assessment of 1C2-positive cells in scrotal skin was performed as described previously.[17] In brief, the frequency of diffuse nuclear staining was calculated from counts of more than 500 nuclei in 5 randomly selected fields of each section (BX51TF; Olympus, Tokyo, Japan). To assess the nuclear accumulation of mutant AR in spinal cord motor neurons, we prepared at least 100 serial transverse sections from the cervical spinal cord and immunostained every 10th section with the anti-polyglutamine 1C2 antibody. For the purposes of counting, a neuron was defined by the presence of its obvious nucleolus in a given 6μm-thick section. The numbers of 1C2-positive and -negative cells within the ventral horn on both the right and left sides were counted under the light microscope with a computer-assisted image analyzer (BX51TF; Olympus), as described previously.[16,35,36] For quantification of 1C2-positive neurons within the pontine base, the frequency of diffuse nuclear staining was calculated from counts of more than 500 neurons in a total of 50 or more fields from each section (BX51N-34; Olympus), as described previously.[37] Populations of 1C2-positive cells were expressed as percentages of the total cell counts.

Autopsy Study

Autopsy specimens of cervical spinal cord (seven patients) and pons (five patients) were obtained from nine control, genetically confirmed SBMA patients who had not participated in any therapeutic trials (52–83 years old; men; 41–52 CAG repeats) and one subject (70 years old) who died at week 67 of the 96-week follow-up study (Patient 16), who had been allocated to the leuprorelin group in the 48-week RCT and had continued leuprorelin administration in the 96-week follow-up trial. The last administration of leuprorelin acetate was at week 60 of the follow-up trial. The causes of death of the control patients were pneumonia in three, respiratory failure in three, unknown in two, and lung cancer in one. Immunohistochemistry of the specimens was performed as described earlier. The collection of tissues and their use for this study were approved by the Ethics Committee of Nagoya University Graduate School of Medicine.

Genetic Analysis

Genomic DNA was extracted from peripheral blood of the patients using conventional techniques, and the CAG repeat size was determined as described previously.[9,11,38] In brief, polymerase chain reaction amplification of the CAG repeat in exon 1 of the *AR* gene was performed using a fluorescein-labeled forward primer (5′-TCCAGAATCTGTTCCAGAGCGTGC-3′) and a nonlabeled reverse primer (5′-TGGCCTCGCTCAGGATGTCTTTAAG-3′). Size of the CAG repeat was analyzed using Fraglys software version 2.2 (Hitachi Electronics Engineering, Tokyo, Japan) by comparison with coelectrophoresed polymerase chain reaction standards with known repeat sizes. Patients with 38 or more CAGs were diagnosed with SBMA.[10] All patients gave their written informed consent to genetic analyses.

Statistical Analyses

The effectiveness analysis and safety evaluation were conducted on data from the intention-to-treat population in the 48-week RCT. We analyzed the data by Pearson's coefficient, Spearman's rank correlation, and Student's t test. The Mann–Whitney U test was used to analyze serum testosterone levels. p values less than 0.05 were considered indicative of significance. For multiple comparisons, p values were corrected using the Dunnett test. Computations were performed with SPSS software (version 14.0J for Windows; SPSS Japan, Tokyo, Japan).

Ethics

This study was conducted according to the Declaration of Helsinki (Hong Kong Amendment). Written informed consent was obtained from each patient. Patients were free to withdraw from the study at any time for any reason. The protocol was approved by the Nagoya University Hospital Institutional Review Board. Confidentiality was ensured by assigning a study code to each patient. All studies conformed to the ethics guidelines for human genome/gene analysis research and the ethics guidelines for epidemiological studies endorsed by the Japanese government.

Results

Demographics

Fifty participants met the eligibility criteria, gave informed consent, and were assigned to either the leuprorelin or placebo group. There were no significant differences in the characteristics of the two groups (Table 1). There were no protocol deviations, although one patient in the leuprorelin group discontinued the drug after 16 weeks because of the patient's schedule, but this patient was included in the end-point analyses.

Table 1. **Characteristics of Patients in the 48-Week Randomized Controlled Trial (RCT)**

Characteristics	Leuprorelin (n = 25)	Placebo (n = 25)	*p*
Mean age ± SD, yr	52.8 ± 7.4	52.0 ± 8.9	NS
Mean height ± SD, cm	167.5 ± 6.2	168.1 ± 6.1	NS
Mean weight ± SD, kg	58.4 ± 5.7	60.2 ± 6.2	NS
Mean duration of weakness ± SD, yr	10.8 ± 6.3	12.9 ± 8.2	NS
Mean (CAG)n ± SD	48.5 ± 3.2	48.1 ± 2.5	NS
Mean ALSFRS-R score ± SD (Japanese edition)	41.1 ± 3.7	42.0 ± 3.4	NS
ADL (cane-assisted/independent)	6/19	7/18	NS

SD = standard deviation; NS = not significant; (CAG)n = number of expanded CAG repeats in the *androgen receptor* gene; ALSFRS-R = revised amyotrophic lateral sclerosis functional rating scale; ADL = activities of daily living.

No patients discontinued treatment prematurely because of adverse events during the 48-week RCT. At the end of the 48-week RCT, 34 of the 50 patients elected to receive leuprorelin administration in the follow-up trial before the key was broken. During this 96-week follow-up trial, one patient discontinued treatment mainly because of depression but was followed up without leuprorelin administration. One patient (Patient 16) died of acute cardiac failure at week 67 and was not included in the end-point analyses (see Fig 1).

Forty-eight-Week Randomized Controlled Trial

The outcome measures of the 48-week RCT are shown in Figure 2. In patients who received leuprorelin acetate, serum testosterone levels decreased to near zero within 4 weeks of the treatment (see Fig 2A). In the placebo group, ALSFRS-R scores had declined by 0.9 point at week 48, suggesting that the change in motor function of patients in this trial was similar to that in a previous study on the natural history of SBMA.[39] Although there was no significant difference in the changes in ALSFRS-R *total* scores at week 48 in the leuprorelin and placebo groups (see Fig 2B), there was a tendency for the swallowing subscores to be improved in the leuprorelin group (see Fig 2C). This view was supported by the fact that the cricopharyngeal opening duration was significantly extended in the leuprorelin group compared with the placebo group, suggesting that androgen deprivation suppressed deterioration of swallowing function in SBMA ($p < 0.05$; see Fig 2D). The serum level of creatine kinase, a marker of muscular involvement in SBMA, and those of liver enzymes also tended to be decreased in the leuprorelin group (see Fig 2E; see Supplemental Table 3). Diffuse nuclear staining was predominantly observed in the scrotal skin biopsy. The frequency of 1C2-positive cells in the scrotal epithelium was significantly decreased at week 48 in the leuprorelin group ($p < 0.001$; see Fig 2F). There were no significant effects of leuprorelin acetate on all other secondary end points (see Supplemental Table 3). Although we performed stratified analyses, neither CAG repeat size nor age had any influence on the outcome measures (data not shown).

Ninety-six-Week Follow-up Trial

All but one patient, who discontinued treatment early in the 48-week RCT, underwent an additional 96-week follow-up. Fifteen patients declined to continue leuprorelin administration mostly because of economic reasons. As shown in Table 2, at the time of enrollment in the follow-up trial, there were no differences in the characteristics of patients who participated and those who were not enrolled, indicating no selection bias for the enrollment.

In the follow-up trial, we compared ALSFRS-R scores and VF findings of the following groups: Group A—patients who were allocated to the leuprorelin group for 48 weeks and received leuprorelin for an additional 96 weeks; Group B—patients who were allocated to the placebo group and received leuprorelin for an additional 96 weeks; Group C—patients who were allocated to the leuprorelin group for 48 weeks but did not receive treatment during the 96-week follow-up; and Group D—patients who were allocated to the placebo group and were followed up without leuprorelin treatment for 96 weeks. Multiple comparisons were performed with Group D as the control. We did not include the following two subjects in these analyses: one patient in Group A who died during the follow-up period and one in Group C who was diagnosed with multiple myelomas during the follow-up period. At week 96 of the follow-up trial, ALSFRS-R scores were significantly greater in Groups A and B than in Group D (Figs 3A, B). Similarly, the swallowing subscores of the ALSFRS-R were significantly greater in Group A than in Group D (see Fig 3C). Cricopharyngeal opening duration in VF was also significantly longer in Groups A and B than in Group D (see Fig 3D).

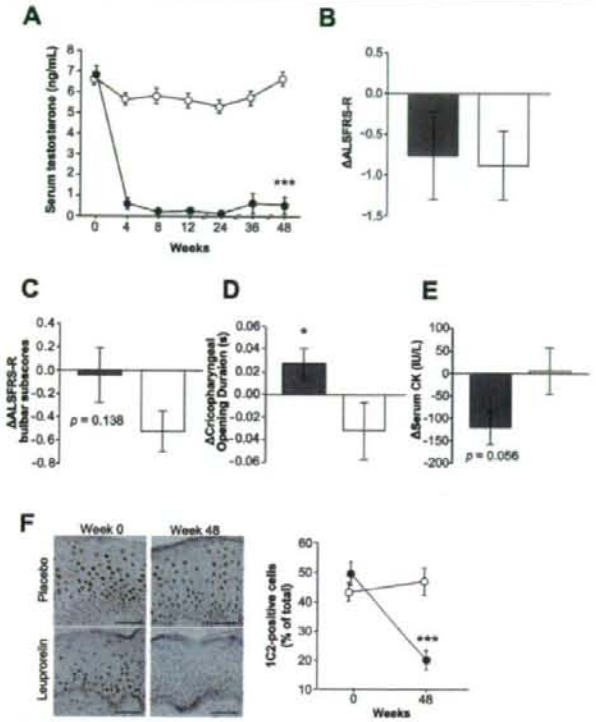

Fig 2. Efficacy results of the 48-week randomized controlled trial (RCT). (A) Treatment with leuprorelin acetate (black circles) *rapidly depleted serum testosterone levels.* White circles *represent placebo group. (B) There was no significant difference in the change in Revised Amyotrophic Lateral Sclerosis Functional Rating Scale (ALSFRS-R) score between the groups. (C) There was a favorable tendency in the swallowing subscores of the ALSFRS-R in the leuprorelin group. (D) Cricopharyngeal opening duration was significantly extended by the 48-week leuprorelin treatment. (E) Serum creatine kinase (CK) levels also tended to be decreased in the leuprorelin group. (F) The frequency of diffuse nuclear 1C2 staining (indicative of mutant androgen receptor [AR]) in the scrotal epithelial cells was significantly decreased after the 48-week administration of leuprorelin acetate.* White bars *represent placebo group;* black bars *represent leuprorelin acetate group. Scale bars = 50μm. Data are expressed as means ± standard error of the mean.* $^{*}p < 0.05$; $^{***}p < 0.001$.

Safety and Tolerability

There were a total of 58 adverse events recorded during the 48-week RCT; none was so serious as to require hospitalization (Table 3). The most frequent adverse event in the leuprorelin group was a loss of sexual function, recorded as erectile dysfunction, but this symptom was also often seen in the placebo group, suggesting androgen insensitivity in SBMA patients. Although increases in total cholesterol, triglyceride, fasting blood sugar, or glycosylated hemoglobin (HbA1c) were seen in the leuprorelin group, no marked exacerbations were observed. The details of adverse events during the 96-week follow-up trial were obtained from Groups A, B, and D. As shown in Table 4, there were no treatment duration–dependent adverse effects of leuprorelin acetate as reported previously.[40]

Autopsy Study

One participant (Patient 16) who received leuprorelin acetate in the 48-week RCT and continued to receive leuprorelin acetate in the 96-week follow-up trial died 118 weeks after initiation of the treatment. Autopsy of the patient indicated acute cardiac failure caused by cardiac arrhythmia as a possible cause of death. Otherwise, no specific causes of death were reported. Autopsied specimens were assessed by anti-polyglutamine (1C2) immunohistochemistry as in the scrotal skin biopsy and were compared with the findings of previously autopsied SBMA cases who had not been treated with leuprorelin acetate or with relevant drugs. In the spinal motor neurons, diffuse nuclear staining of 1C2 was predominantly observed, and nuclear inclusions were less frequent. The frequencies of 1C2-positive

Table 2. **Characteristics of Patients in the 96-week Follow-up Trial**

Treatment in 96-week Follow up	Leuprorelin in 48-week RCT (n = 22)			Placebo in 48-week RCT (n = 25)		
	Leuprorelin (Group A, n = 18)	No Treatment (Group C, n = 4)	*p*	Leuprorelin (Group B, n = 15)	No Treatment (Group D, n = 10)	*p*
Age (yr)	52.0 ± 6.5	56.3 ± 8.1	NS	52.5 ± 8.2	51.3 ± 10.2	NS
Height (cm)	168.6 ± 5.8	164.3 ± 9.4	NS	168.5 ± 5.0	167.6 ± 7.7	NS
Weight (kg)	58.6 ± 5.9	58.8 ± 6.2	NS	59.6 ± 5.6	61.2 ± 7.3	NS
Duration of Weakness (yr)	11.7 ± 6.4	8.3 ± 7.4	NS	12.8 ± 5.5	13.0 ± 11.5	NS
(CAG)n	49.1 ± 3.3	45.8 ± 2.2	NS	48.0 ± 2.5	48.2 ± 2.6	NS
ALSFRS-R (Japanese Edition) *	41.3 ± 2.8	40.5 ± 7.7	NS	42.1 ± 2.6	42.0 ± 4.5	NS
	41.2 ± 3.7	39.8 ± 6.7	NS	40.7 ± 3.6	41.9 ± 5.0	NS
ADL (cane-assisted/independent) *	3/15	1/3	NS	4/11	3/7	NS
	7/11	2/2	NS	6/9	3/7	NS

*Upper values indicate data at inclusion in the 48-week RCT, and lower values those at inclusion in the 96-week follow-up trial. Other values are data at inclusion of 48-week RCT. (CAG)n = number of expanded CAG repeats in the *androgen receptor* gene; ALSFRS-R = revised amyotrophic lateral sclerosis functional rating scale. Data represent means ± SD except for ADL.

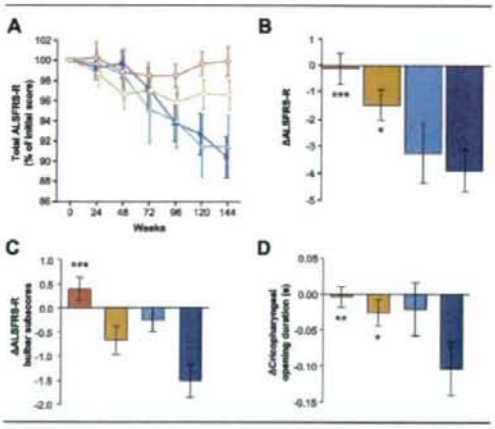

*Fig 3. Efficacy results of the 96-week follow-up trial. (A, B) Changes in the Revised Amyotrophic Lateral Sclerosis Functional Rating Scale (ALSFRS-R) scores showed treatment duration–dependent improvements in the leuprorelin-treated groups. (C, D) The ALSFRS-R bulbar subscores (C) and videofluorography (VF) findings (D) were also significantly improved in the leuprorelin-treated patients. Data are expressed as means ± standard error of the mean. *p < 0.05; **p < 0.005; ***p < 0.001 with respect to Group D. Red represents Group A: 48-week leuprorelin/96-week leuprorelin (n = 18); orange represents Group B: 48-week placebo/96-week leuprorelin (n = 15); light blue represents Group C: 48-week leuprorelin/96-week no treatment (n = 4); blue represents Group D: 48-week placebo/96-week no treatment (n = 10).*

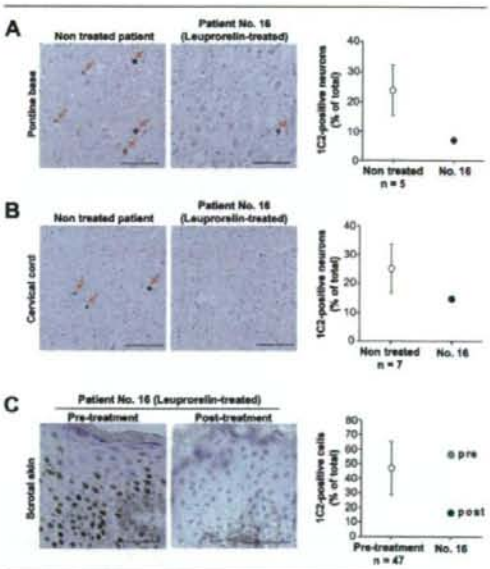

Fig 4. Effects of leuprorelin acetate on nuclear accumulation of mutant androgen receptor (AR). (A, B) Accumulation of mutant AR in neurons was remarkable both in the pontine base and in the spinal anterior horn of all the control, non-treated autopsied cases, but the number of 1C2-positive neurons was relatively small in the leuprorelin-treated patient (Patient 16). Scale bars = 100μm. (C) Mutant AR accumulation in scrotal skin epithelial cells that underwent biopsy was markedly reduced by leuprorelin acetate in Patient 16 (Patient 16 was excluded from this mean.) Scale bars = 50μm. Data are expressed as means ± standard deviation.

Table 3. **Adverse Events in 48-Week Randomized Controlled Trial**

AEs	Leuprorelin (n = 25)	Placebo (n = 25)
At least one AE	21 (84%)	9 (36%)
At least one AE other than ED	16 (64%)	6 (24%)
ED[a]	13 (52%)	4 (16%)
Hypertriglyceridemia	7 (28%)	0
Lumbago	5 (20%)	1 (4%)
Headache	5 (20%)	1 (4%)
Numbness	3 (12%)	2 (8%)
Hand arthralgia	4 (16%)	0
Fatigue	3 (12%)	0
Hot flush	3 (12%)	0
Injection site lump	3 (12%)	0
Hypertension	2 (8%)	0
Fracture	0	2 (8%)

[a]Number was calculated by questionnaire on every visit. AE = adverse event; ED = erectile dysfunction.

neurons in the anterior horn and brainstem of Patient 16 were less than those in non-treated SBMA patients (Figs 4A, B). By way of comparison, the pretreatment frequency of 1C2-positive cells in the biopsied scrotal skin of Patient 16 was a little higher than the mean value of other study participants at week 0 but decreased after 48 weeks of leuprorelin treatment in the RCT (see Fig 4C). Hence, this patient's pretreatment frequency of 1C2-positive cells in the anterior horn and brainstem were presumed to also be greater than the posttreatment levels.[17]

Discussion

Recent research on neurodegenerative diseases has repeatedly shown that abnormal protein accumulation in neuronal cells is important in the molecular pathogenesis of neurodegeneration.[41] In polyglutamine diseases including SBMA, the aberrant proteins that contain an extended polyglutamine tract accumulate chiefly in the nucleus, resulting in the disruption of cellular functions such as transcription.[14,42] To date, no disease-modifying therapies for polyglutamine diseases have proved beneficial in clinical trials. The results of this interventional trial suggest that androgen deprivation therapy for SBMA is a promising therapy targeting the molecular pathogenesis of polyglutamine diseases.

In this study, we demonstrated that leuprorelin acetate suppressed toxic accumulation of the mutant AR protein, and thereby slowed down the progression of SBMA. As shown previously in animal and human studies, leuprorelin-mediated androgen deprivation significantly decreased mutant AR accumulation in scrotal skin.[17,21] Furthermore, our histopathological analysis in the autopsied case suggests that leuprorelin treatment also attenuates the nuclear accumulation of pathogenic AR within neuronal cells. AR did not aggregate even in the cytoplasm of scrotal epithelial cells or in that of spinal motor neurons, presumably because androgen deprivation destabilizes AR and facilitates degradation of the protein.[43] Alternatively, androgen deprivation may enhance the protective effects of heat shock proteins, which are normally associated with AR and dissociate on ligand binding.

The 48-week treatment with leuprorelin acetate significantly extended cricopharyngeal opening duration, indicating that this therapy blocked disease progression measured with the most reliable VF parameter. The opening of the cricopharyngeal sphincter is triggered by the motion of the larynx and is widened by pharyngeal pressure.[44] Therefore, cricopharyngeal opening duration reflects the strength of deglutition and has been used as a quantitative parameter of swallowing function in disease conditions such as stroke and inflammatory myopathy.[45,46] Moreover, in patients with ALS, cricopharyngeal opening duration is shortened as a consequence of delayed opening or premature closure of the cricopharyngeal sphincter, or both, and this shortening correlates well with the severity of dysphagia.[47] The amelioration of dysphagia by androgen deprivation is also supported by the 96-week follow-up trial, in which leuprorelin treatment significantly prolonged cricopharyngeal opening duration and improved the bulbar subscores of the ALSFRS-R. Given that pneumonia and respiratory distress are the main causes of death in this disease, leuprorelin treatment appears to be beneficial for the prognosis of SBMA patients.[7]

Although the effect of leuprorelin acetate on general motor function was not clear in the 48-week RCT, the total ALSFRS-R score was significantly greater in patients who received androgen deprivation therapy for 144 or 96 weeks than in those who received no therapy throughout the trial. Although the total ALSFRS-R score is a reliable marker of the progression of ALS, this score is less sensitive for SBMA.[39,48] This study suggests that the ALSFRS-R score is not an appropriate end point in a short-term trial but may be useful in a long-term clinical trial on SBMA.

No unexpected or serious safety issues associated with the long-term use of leuprorelin acetate were identified during this study. The adverse effects of leuprorelin acetate did not differ from those in trials for prostate cancer.[49,50] Although erectile dysfunction after leuprorelin administration was more frequent in this trial than in previous trials for prostate cancer, this is likely because of pre-existing androgen insensitivity in

Table 4. **Adverse Events during Leuprorelin Administration (48-Week Randomized Controlled Trial and 96-Week Follow-up)**

AEs	Group A (n = 19)[a]	Group B (n = 15)	Group D (n = 10)
At least one AE	18 (95%)	15 (100%)	7 (70%)
At least one AE other than ED	15 (79%)	11 (73%)	5 (50%)
ED[b]	13 (68%)	9 (60%)	2 (20%)
Numbness	7 (37%)	3 (20%)	2 (20%)
Arthralgia	5 (26%)	5 (33%)	1 (10%)
Hot flush	5 (26%)	4 (27%)	0
Injection-site lump	5 (26%)	4 (27%)	0
Lumbago	5 (26%)	1 (7%)	1 (10%)
Myalgia	2 (11%)	2 (13%)	0
Edema	3 (16%)	0	0
Headache	3 (16%)	0	1 (10%)
Fatigue	2 (11%)	1 (7%)	0
Hyperglycemia	2 (11%)	1 (7%)	1 (10%)
Hypertension	1 (5%)	1 (7%)	0
Death	1 (5%)	0	0
Neuralgia	1 (5%)	0	0
Pollakiuria	1 (5%)	0	0
Depression	0	1 (7%)	0
Fracture	0	1 (7%)	1 (10%)
Hyperlipidemia	0	1 (7%)	1 (10%)

[a]All patients were analyzed including Patient 16. [b]Number was calculated by questionnaire on every visit. AE = adverse event; ED = erectile dysfunction.

SBMA.[51] The high tolerability of leuprorelin acetate was also supported by the low dropout rate in this trial.

An important limitation in this study is the trial duration. SBMA is a slowly progressive disease, with a disease duration of approximately 20 years.[7] Given that leuprorelin acetate did not suppress the decline in ALSFRS-R scores in our 48-week RCT, a long-term, placebo-controlled trial may be necessary to evaluate the efficacy of leuprorelin acetate on general motor function in SBMA. Based on this study, cricopharyngeal opening duration in VF appears to be a practical biomarker to evaluate therapy efficacy for SBMA in short-term trials.

In conclusion, the results of this study suggest that leuprorelin acetate administration suppresses nuclear accumulation, stabilization, or both of mutant AR, the causative protein of SBMA, and appears to inhibit functional deterioration of the patients. The results of this phase 2 trial support the start of large-scale clinical trials of androgen deprivation for SBMA.

This study was supported by the Ministry of Education, Culture, Sports, Science and Technology, Japan (17025020, 19209033, G.S.; 20390243, H.A.); the Ministry of Health, Labor and Welfare, Japan (Health and Labor Sciences Research Grants H18YO022, H20YP015, CCT-B-1701, CCT-C-1810, G.S.); and the Program for Improvement of Research Environment for Young Researchers from Special Coordination Funds for Promoting Science and Technology (SCF) commissioned by the Ministry of Education, Culture, Sports, Science and Technology of Japan (M.K.).

Acknowledgments

We thank Drs Y. Ohmae, F. Ohshima, N. Katayama, and A. Tamakoshi for technical advice. M. Mendoza kindly gave instruction in maximum voluntary isometric contraction testing. Dr Y. Hasegawa provided patient information. We acknowledge and thank all patients and their families for participating in this study.

References

1. Kennedy WR, Alter M, Sung JH. Progressive proximal spinal and bulbar muscular atrophy of late onset. A sex-linked recessive trait. Neurology 1968;18:671–680.
2. Sperfeld AD, Karitzky J, Brummer D, et al. X-linked bulbospinal neuronopathy: Kennedy disease. Arch Neurol 2002;59:1921–1926.
3. Sobue G, Hashizume Y, Mukai E, et al. X-linked recessive bulbospinal neuronopathy. A clinicopathological study. Brain 1989;112(pt 1):209–232.